

**Bioglass 45S5 transformation and molding material
in the processing of biodegradable poly-DL-lactide
scaffolds for bone tissue engineering**

Sara Abdollahi

Department of Mining and Materials Engineering

McGill University, Montréal

December 2011

A thesis submitted to McGill University in partial fulfillment of the
requirements of the degree of Master of Engineering

© Sara Abdollahi 2011

Table of Contents

ABSTRACT.....	i
RÉSUMÉ.....	iii
ACKNOWLEDGEMENTS.....	v
LIST OF FIGURES.....	vi
LIST OF TABLES.....	viii
GLOSSARY OF ABBREVIATIONS.....	ix
1 – INTRODUCTION.....	1
1.1 INTRODUCTION & RESEARCH RATIONALE.....	2
1.2 OBJECTIVES OF THESIS.....	3
1.3 ORGANIZATION OF THESIS.....	4
2 – LITERATURE REVIEW.....	6
2.1 BONE TISSUE ENGINEERING.....	7
2.1.1 <i>Tissue Engineering & Artificial Extracellular Matrices</i>	7
2.1.2 <i>Bone</i>	9
2.1.3 <i>Characteristics of Scaffolds in Bone Tissue Engineering</i>	14
2.1.4 <i>Scaffold Materials for Bone Tissue Engineering</i>	16
2.1.5 <i>Scaffold Fabrication Techniques</i>	24
2.2 MOLDING MATERIAL.....	27
2.2.1 <i>Teflon</i>	27
2.2.2 <i>Sil940</i>	29
2.2.3 <i>Polyurethane</i>	29
2.2.4 <i>Polyether</i>	30
2.2.5 <i>Polydimethylsiloxane</i>	31
3 – METHODOLOGY.....	32
3.1 MATERIALS.....	33
3.2 COMPOSITE PDLA-BIOGLASS SCAFFOLDS.....	34
3.2.1 <i>Characterizations</i>	34
3.2.2 <i>Bioglass 45S5 Preliminary Analysis</i>	37
3.2.3 <i>Scaffold Processing</i>	39
3.2.4 <i>Bioglass45S5 Scaffold Extraction</i>	42
3.3 MOLD PREPARATION.....	42
4 – RESULTS & DISCUSSION.....	48
4.1 BIOGLASS 45S5 TRANSFORMATION.....	49
4.1.1 <i>Bioglass 45S5 Preliminary Characterization</i>	49
4.1.2 <i>Scaffold Characterization & the Effect of Bioglass 45S5 Addition</i>	56
4.1.3 <i>Bioglass 45S5 Transformation in Scaffold Processing</i>	57
4.2 MOLD MATERIAL FOR SCAFFOLD DESIGN.....	66
5 – CONCLUSION & SUMMARY.....	76
5.1 BIOGLASS 45S5 TRANSFORMATION.....	77
5.2 MOLDING MATERIAL.....	78
5.3 SUGGESTIONS FOR FUTURE WORK.....	79
6 – REFERENCES.....	81

7 – APPENDICES	85
APPENDIX A: BIOGLASS 45S5 PARTICLE SIZING.....	86
APPENDIX B: XPS CHARACTERIZATION OF MOLDING MATERIALS	91

Abstract

When bone is damaged, a scaffold can temporarily replace it in the site of injury and incite bone tissue to repair itself. A biodegradable scaffold resorbs into the body, generating non-toxic degradation products as new tissue reforms; a bioactive scaffold encourages the surrounding tissue to regenerate. In the present study, we make composite biodegradable and bioactive scaffolds using poly-DL-lactide (PDLLA), a biodegradable polymer, and incorporate Bioglass 45S5 (BG) to stimulate scaffold bioactivity. BG has an interesting trait when immersed in body fluid, a layer of hydroxycarbonate apatite, similar to the inorganic component of bone, forms on its surface. It is of utmost importance to understand the fate of BG throughout the scaffold's processing in order to assess the scaffold's bioactivity.

In this study, the established different stages of BG reactivity have been verified by monitoring pH during BG dissolution experiments and by conducting an elemental analysis using inductively coupled plasma optical emission spectroscopy (ICP-OES). The composite scaffolds are synthesized by the solvent casting and particulate leaching technique and their morphology assessed by scanning electron microscopy (SEM). To understand the transformations occurred in BG during scaffold synthesis, BG as received, as well BG treated in acetone and water (the fluids involved in scaffold processing) are characterized by Fourier transform infrared (FTIR), and x-ray photoelectron spectroscopy (XPS). The results are then compared with BG extracted from scaffolds after processing. BG has been determined to start reacting during the scaffold processing. In addition, its

reactivity is influenced by BG particle size. The study suggests that the presence of the polymer provides a reactive environment for BG due to pH effects.

Teflon molds in scaffold fabrication are inert and biocompatible, but their stiffness presents a challenge during de-molding. Silicone-based and polyurethane molds are attractive because they are flexible. However, there is a possibility that silicone leaches either from the material itself or the agents used to enhance their performance onto the scaffold. The second study in this thesis focuses on different types of such flexible substrates (Sil940, polyurethane, polyether, polydimethylsiloxane). The presence of Si in PDLLA films prepared on each material is inspected using XPS. Films made on all four materials are found to contain Si, indicative of the dissolution of part of the substrate in the film. However, silicon in the Si-containing catalysts used in the synthesis of polyethers is not transferred to samples, when the polyether substrate is plasma coated.

Résumé

Quand l'os est endommagé, une matrice synthétique peut le substituer temporairement et encourager la reconstruction du tissu osseux. Une matrice biodégradable résorbe dans le corps, engendrant des produits de dégradation non toxique alors que de le nouveau tissu se réformé. Dans la présente étude, on fabrique un composé biodégradable et bioactifs en utilisant poly(D,L-acide lactique) (PDLLA), un polymère biodégradable, et en incorporant Bioglass 45S5 (BG) pour stimuler la bioactivité. BG est un verre à base de silice qui lors du contact avec les fluides corporels, se dissout et libère des ions de silice, phosphate, calcium et sodium. Les ions de calcium et phosphate reprécipitent et forment une couche d'hydroxycarbonate apatite sur la surface du BG, qui ressemble le composant inorganiques de l'os. Puis, la couche d'hydroxycarbonate apatite s'intègre avec le collagène fibrillaire des tissus environnants, le composant organique de l'os, pour former une matrice qui attire les ostéoblastes et stimule l'accroissement du tissu osseux.

Ce composite biosynthétique est développé avec la méthode de fusion du sel et sa morphologie est déterminée avec la microscopie électronique à balayage (MEB). Pour évaluer la bioactivité de l'échafaudage, il est important de comprendre le sort du BG durant la production de la matrice. Les différents stages de la réactivité du BG ont été vérifiés en surveillant le pH durant la dissolution du BG et conduisant une analyse élémentaire par la spectrométrie d'émission optique à plasma à couplage inductif (ICP-OES). Pour comprendre les transformations du BG lors de la synthèse des matrices, le BG tel que reçu avec le BG traités dans l'acétone et l'eau (les fluides impliqués dans la procédure de la synthèse) sont caractérisées avec la spectroscopie infrarouge à

transformée de Fourier (FTIR) et la spectrométrie photoélectronique X (XPS). Les résultats sont par la suite comparés avec ceux du BG extrait des matrices. Nous avons déterminées que BG réagit durant la préparation de la matrice. De plus, la réactivité du BG est influencée par la grandeur ses particules. La présence du polymère crée un milieu réactif pour le BG, ce qui est due à l'effet du pH.

La moule en Teflon utilisée dans la fabrication des matrices biosynthétique est inerte et biocompatible, mais aussi rigide, ce qui peut être problématique durant l'extraction. Ceci engendre une autre investigation qui implique la recherche d'une moule malléable pour faciliter l'enlèvement de la matrice. Les moules à base de silicone et polyuréthane sont attirantes parce qu'elles sont flexibles. Pourtant, il y a une possibilité que la silicone qui fait partie du matériel ou présent dans les produits utilisées pour augmenter sa performance se retrouve sur le produit final. Une deuxième étude dans la présente thèse est donc consacrée sur différents substrats flexibles (Sil940, polyuréthane, polyéther, polydimethylsiloxane). Le XPS est utilisé pour inspecter des films de PDLLA produit sur chaque matériel. La silicone est présente dans les films préparés sur tous les quatre matériaux. Cependant, lorsque le plasma est appliqué pour recouvrir le polyéther, la silicone présente dans les catalyses utilisées pour sa fabrication n'est pas transmises sur celui-ci. Donc le polyéther traité avec le plasma est convenable pour la fabrication des matrices biosynthétiques extracellulaires.

Acknowledgements

I express gratitude to my thesis advisor, Prof. Marta Cerruti, who has given me continuous guidance throughout this project. It is a pleasure to be part of the Biointerface lab group.

I acknowledge the financial support during the present study from *Fonds Québécois de la Recherche sur la Nature et les Technologies (FQRNT)*. I thank *NovaBone Products, LLC* and *Boehringer Ingelheim Chemicals, Inc.* for kindly providing materials necessary to carry out this project. I am grateful to have been awarded the *Provost Graduate Fellowship*, and *Graduate Research Enhancement and Travel (GREAT) Award* during my studies in McGill University's Department of Mining and Materials Engineering.

I would like to acknowledge Dr. Sylvain Coulombe, Dr. Faleh Tamimi, and Dr. Martin Koch for their assistance, advice, support and collaboration at different stages of the project. I thank Helen Campbell and Monique Riendeau for their technical support and training of various laboratory instruments. I am also grateful to have been granted access to the Chemical Engineering laboratory facilities and the assistance of Mr. Ranjan Roy and Mr. Andrew Golsztajn in some of the experiments during the study.

Finally and most importantly, I am grateful to my parents and sister for always cheering me throughout all my endeavours.

List of Figures

- Fig. 2.1 – The Tissue Engineering Concept Map
- Fig. 2.2 – Bone
- Fig. 2.3 – Collagen fibrils and minerals crystals arrangement in bone
- Fig. 2.4 – Bone development: endochondral ossification
- Fig. 2.5 – Synthetic pathway for PLA synthesis
- Fig. 2.6 – Synthetic pathway for PGA synthesis
- Fig. 2.7 – Chemical steps to PGA or PLA
- Fig. 2.8 – PLA and PGA structures
- Fig. 2.9 – Degradation Rates of Biomedical Polyesters
- Fig. 2.10 – Degradation Product of PLLA
- Fig. 2.11 – PLGA Synthesis
- Fig. 2.12 - Degradation Product of PLGA
- Fig. 2.13 – Stages of Bioglass 45S5 reactivity
- Fig. 2.14 – Haemoglobin free test on collagen, Teflon and glass (a); fibrin formation (b); thrombogenicity index (c).
- Fig. 2.15 – Snap-Set Time: Polyether vs. Silicone
- Fig. 3.1 – Preliminary Bioglass 45S5 Analysis Scheme
- Fig. 3.2 – Porogen Range for Scaffold Pore Size
- Fig. 3.3 – Scaffold Preparation by Solvent Casting/Particulate Leaching
- Fig. 3.4 – Scaffold Molding Step
- Fig. 3.5 – PDLLA Film on Teflon Mold Substrate
- Fig. 3.6 – Coating Sil940 Substrate with Lacquer
- Fig. 3.7 – Teflon Spray Coating for Sil940 Substrate
- Fig. 3.8 – Sil940 Covered with PTFE Tape: PDLLA (a), and PDLLA/NaCl (b) films
- Fig. 3.9 – PDLLA Film Preparation on Polyurethane Substrate
- Fig. 3.10 – Polyether Substrate: chemical formula (a), and PDLLA Film Preparation (b)
- Fig. 4.1 – Bioglass 45S5 Particle Size Analysis: Mean Particle Size (M.P.S.) and Standard Deviations of as received, 2 days water, 2 days acetone, and 2 days both water and acetone treatments (S.D.)
- Fig. 4.2 – FTIR transmission spectra of BGA: as received (black), after acetone treatment (red), and after both acetone and water treatments (blue)

Fig. 4.3 – FTIR transmission spectra of silica doped with: sodium (red), and calcium (blue)

Fig. 4.4 – pH effects of Bioglass 45S5 dissolution

Fig. 4.5 – Bioglass 45S5 ion exchange in solution

Fig. 4.6 – SEM image of PDLLA scaffold prepared using the solvent casting/particulate leaching technique with BGA

Fig. 4.7 – FTIR spectra of scaffold: PDLLA matrix only (black), and Composite PDLLA/BGA scaffolds

Fig. 4.8 – FTIR spectra of BGA: as received (black), 2 days acetone treated (red), and extracted from the scaffold (blue)

Fig. 4.9 – Chemical environment of Si in Bioglass 45S5 at different stages of reactivity

Fig. 4.10 – Stages of Bioglass 45S5 reactivity

Fig. 4.11 – FTIR spectra of BGB: as received (black), 2 days acetone treated (red), and extracted from the scaffold (blue)

Fig. 4.12 – XPS spectra for phosphorus of BGA: as received (black), treated (red), and extracted (blue)

Fig. 4.13 – Phosphorus in pyrophosphate-like environment

Fig. 4.14 – XPS spectra of silicon for BGA: as received (black), treated (red), and extracted (blue)

Fig. 4.15 – The pH effect: Bioglass 45S5 and scaffold dissolution experiments

Fig. 4.16 – Scaffolds Prepared in Teflon Mold

Fig. 4.17 – Scaffold Prepared in Lacquer Coated Sil940 Mold

Fig. 4.18 – Deteriorated Lacquer Coating on Sil940 Mold

Fig. 4.19 – High Resolution XPS Analysis of PDLLA Film Cast on Teflon Spray Coated Sil940

Fig. 4.20 – Sil940 PTFE tape covered scaffold

Fig. 4.21 – XPS Elemental Survey of PDDL film cast on plasma Coated Polyether

Fig. 4.22 – XPS Si High Resolution Spectra of PDLLA film on plasma Coated Polyether

Fig. 4.23 – Scaffold Prepared in PDMS Mold

Fig. 4.24 – XPS High Resolution Si Spectra with Etching (~1 nm/s) on PDDLs film prepared on ethanol treated PDMS substrate

List of Tables

Table 2.1 – Characteristics of the ideal scaffold

Table 2.2 – Properties of synthetic biodegradable polymers

Table 2.3 – ReoFlex® Urethane Rubber Properties

Table 3.1 – ICP emission lines

Table 4.1 – As received BG Particle Size

Table 4.2 – BGA “2 days water immersion” water

Table 4.3 – BGB “2 days water immersion” water

Table 4.4 – BGA “2 days acetone, 2 days water immersion” water

Table 4.5 – BGB “2 days acetone, 2 days water immersion” water

Table 4.6 – BG Designations

Glossary of Abbreviations

2D	Two-dimensional
3D	Three-dimensional
At.%	Atomic percent
BG	Bioglass 45S5
BGA	Bioglass 45S5 with average particle diameter of 75 μm (small BG)
BGB	Bioglass 45S5 with average particle diameter of 150 μm (large BG)
ECM	Extracellular matrix
FDA	United States Food and Drug Administration
FTIR	Fourier transform infrared spectroscopy
ICP-OES	Inductively coupled plasma optical emission spectroscopy
HA	Hydroxyapatite
HCA	Hydroxycarbonate apatite
PCL	Polycaprolactone
PDLLA	Poly-DL-lactic acid
PDMS	Polydimethylsiloxane
PGA	Polyglycolic acid
PLA	Poly(lactic acid)
PLGA	Poly(lactic-co-glycolic acid)
PLLA	Poly-L-lactide acid
PTFE	Polytetrafluoroethylene
S.D.	Standard deviation
SEM	Scanning electron microscopy
TIPS	Thermally induced phase separation
XPS	X-ray photoelectron spectroscopy
wt%	Weight percent

1 – Introduction

This chapter provides the rationale behind undertaking research pertaining to Bioglass 45S5 transformation and molding material in the processing of biodegradable poly-DL-lactide scaffolds for bone tissue engineering. The objectives of the work as well as an overall organization of the thesis are also provided.

1.1 Introduction & Research Rationale

An article published in 2000 presents tissue engineering as an emerging alternative to other treatment methods for tissue and organ failure such as transplantation and artificial prosthesis because these do not satisfactorily restore damaged tissue (Persidis, 2000). A decade later, a field seeming to have surfaced from science fiction has gained rapid momentum. Add-on novelties, such as those involving nanotechnology, now enrich the original concept proposed by J. Vacanti and R. Langer to induce tissue self-repair (T. Dvir, Timko, Kohane, & Langer, 2011). The synthesis of a functional tissue that grows within the damaged area involves many factors, such as cells and an appropriate environment where they can thrive and lead new tissue development (Persidis, 2000). A scaffold is a three-dimensional matrix that allows cells to anchor, differentiate and proliferate, thus providing the suitable environment necessary to their survival. When made with biodegradable materials, the structure conveniently gradually degrades as the surrounding tissue matrix re-grows.

Scaffolds for bone tissue engineering must possess a porous structure, similar to bone, to allow nutrients and oxygen to reach the inner cells, and yet be biomechanically stable to sustain load at the site of injury. The marriage of porosity, biodegradability and mechanical strength is best met in a composite material. In fact, bone is also a composite, encompassing both an organic collagenous matrix, and an inorganic mineral component (T. Dvir, et al., 2011). As a result, composite scaffolds combining a polymer and a bioactive glass, such as PDLA and Bioglass 45S5, have been the subject of many

studies (Cerruti, Greenspan, & Powers, 2005; Greenspan & Hench, 1976; Khademhosseini, Vacanti, & Langer, 2009). BG is a silicate-based glass that dissolves when in contact with body fluids, and generates sodium, phosphate, calcium and silicate ions (Cerruti, Greenspan, et al., 2005; Greenspan & Hench, 1976; Hench, Paschall, Paschall, & Mcvey, 1973). Calcium and phosphate ions re-precipitate on the BG surface and form a layer of hydroxyl carbonate apatite. This layer is similar in composition to the inorganic component of bone, and it can thus integrate with the surrounding tissue fibrillar collagen, the organic component of bone, to form a matrix that attracts osteoblasts and incites bone tissue regrowth (Liu & Ma, 2004; Panetta, Gupta, & Longaker, 2009). The properties of the final processed scaffold are at the centerpiece of many studies. However, given the mechanism of BG reactivity, an important question is whether BG starts transforming during the scaffold processing. Furthermore, scaffold processing using the solvent casting/particulate leaching technique requires inert molds, which are often made of Teflon. The rigidity of Teflon molds triggers another investigation, to find an alternative material that is similarly inert, yet flexible.

1.2 Objectives of Thesis

The goal of the present research is to investigate Bioglass 45S5 transformation in the processing of polymeric scaffolds for bone tissue engineering. A concurrent goal is to determine the most suitable moulding material for scaffold fabrication. In reaching these goals, it is necessary to:

1. Understand scaffold applicability within the context of tissue engineering.

2. Review the characteristics and development of bone to determine the properties required for creating a biomimetic artificial bone matrix.
3. Review the most commonly used biodegradable polyester materials and their processing techniques and select the most suitable for evaluating Bioglass 45S5 transformation.
4. Develop composite biodegradable scaffolds for bone tissue engineering.
5. Understand the proposed stages of reactivity of Bioglass 45S5 in body fluid to define the chemical changes that occur on its surface during scaffold synthesis.
6. Characterize the transformation of Bioglass 45S5 during scaffold processing.
7. Study silicone-based moulding materials and characterize them to choose the best fit for making scaffolds using the solvent casting/particulate leaching technique.

1.3 Organization of Thesis

This thesis consists of the current introductory chapter, a literature review (chapters 2), the methodology of the research (chapter 3), along with the results and discussion (chapter 4), followed by a conclusion and summary (chapter 5). Two appendices presenting some of the experimental raw data are provided at the end. A brief description of chapter contents is presented below:

- Chapter 1: Presents a general introduction of the topic at hand and provides the rationale for undertaking this research as well as its objectives.
- Chapter 2: A review of literature is presented, which highlights the interplay of key components involved in creating scaffolds for bone tissue engineering, such as biodegradable polyesters, Bioglass 45S5, and the moulding material.

- Chapter 3: Describes the detailed methodology for (i) fabricating and characterizing PDLLA-Bioglass scaffolds for bone tissue engineering, and (ii) developing moulding materials and analyzing their surface composition for selecting the most appropriate in scaffold processing.
- Chapter 4: Presents and discusses the outcomes of the characterization involved (ICP-OES, particle sizing, FTIR, dissolution experiments, SEM, and XPS) in evaluating both Bioglass 45S5 transformation and moulding materials for processing of PDLLA scaffolds.
- Chapter 5: In addition to providing a summary of the research and conclusions of the study, this chapter provides possible suggestions for future work.
- Chapter 6: Encompasses the comprehensive list of literature referenced in this study.
- Chapter 7: The appendices include some of the key raw data from the studies.

2 – Literature Review

Crucial in this study is to understand the role of scaffolds within the context of bone tissue engineering, bone matrix structure and development, biodegradable polyesters, stages of Bioglass 45S5 reactivity, and potential candidates for moulding material in scaffold processing. This chapter gives an overview of each topic.

2.1 Bone Tissue Engineering

Bone tissue engineering is an area of research under intense investigation. Although much progress has been made in the field, many challenges still remain (Tal Dvir et al., 2011).

This section covers the essential factors to consider in bone tissue reconstruction.

2.1.1 Tissue Engineering

& Artificial Extracellular Matrices

Tissue extracellular matrix (ECM) is not a passive structure, but rather an action zone where cellular phenotypes receive instruction (Streuli, 1999). The ECM takes various forms in different tissues and at different stages of development of the same tissue. The diversity is due in part to the different ratios and geometrical arrangements of the components of the matrix, such as collagen, elastin, proteoglycans, fibronectin and laminin, as well as a result of the molecular interactions between them. ECM proteins have multiple motifs that are encoded by specific sequences of amino acids. These motifs bind to specific cell surface receptors and initiate different intracellular signaling pathways. For instance, the transmembrane integrin receptors recognize motifs, such as Arg-Gly-Asp (RGD) within the proteins of the ECM, for example, vitronectin and fibronectin. At the same time, cell membrane receptors rarely act alone, and for the most part, belong to multi-component systems that enable diverse signal integration (Behonick & Werb, 2003; Bökel & Brown, 2002; Giancotti & Ruoslahti, 1999; Plopper, McNamee, Dike, Bojanowski, & Ingber, 1995; M. M. Stevens & George, 2005; Taipale & Keski-Oja, 1997; Tran, Lamb, & Deng, 2005).

Figure 2.1 depicts the concept map of tissue engineering. When a tissue in the body is damaged, for example during an injury, the ideal strategy is to incite the tissue to self-heal. This could be possible if the cells of the tissue excrete the extracellular matrix components necessary for its reconstruction. However, simply adding osteoblasts to the site of bone loss, for instance, is ineffective because cells cannot sustain themselves without a support matrix, similar to that of the native tissue, to which they can anchor. Thus, in addition to isolating cells from the patient and culturing them in a 2D *in vitro* environment (Fig. 2.1a,b), tissue engineering involves using an artificial extracellular matrix, also called a scaffold, to seed cells (Fig. 2.1c) on a 3D matrix. This structure is a suitable “housing” for the cells and when adequately designed allows them to take up nutrients, proliferate, differentiate, and form tissues (Fig. 2.1d). Scaffolds closely mimicking the properties of the original tissue can be created by incorporating extracellular biomolecules of the native matrix. Including other elements, such as growth factors, is another common practice. In addition, both physical and chemical properties of the scaffold can be adjusted throughout its fabrication. Ultimately, the tissues are transplanted (Fig. 2.1e). Biodegradable polyesters are commonly used to create scaffolds that slowly degrade after implantation as the surrounding tissue gradually regenerates (Tal Dvir, et al., 2011; T. Dvir, et al., 2011).

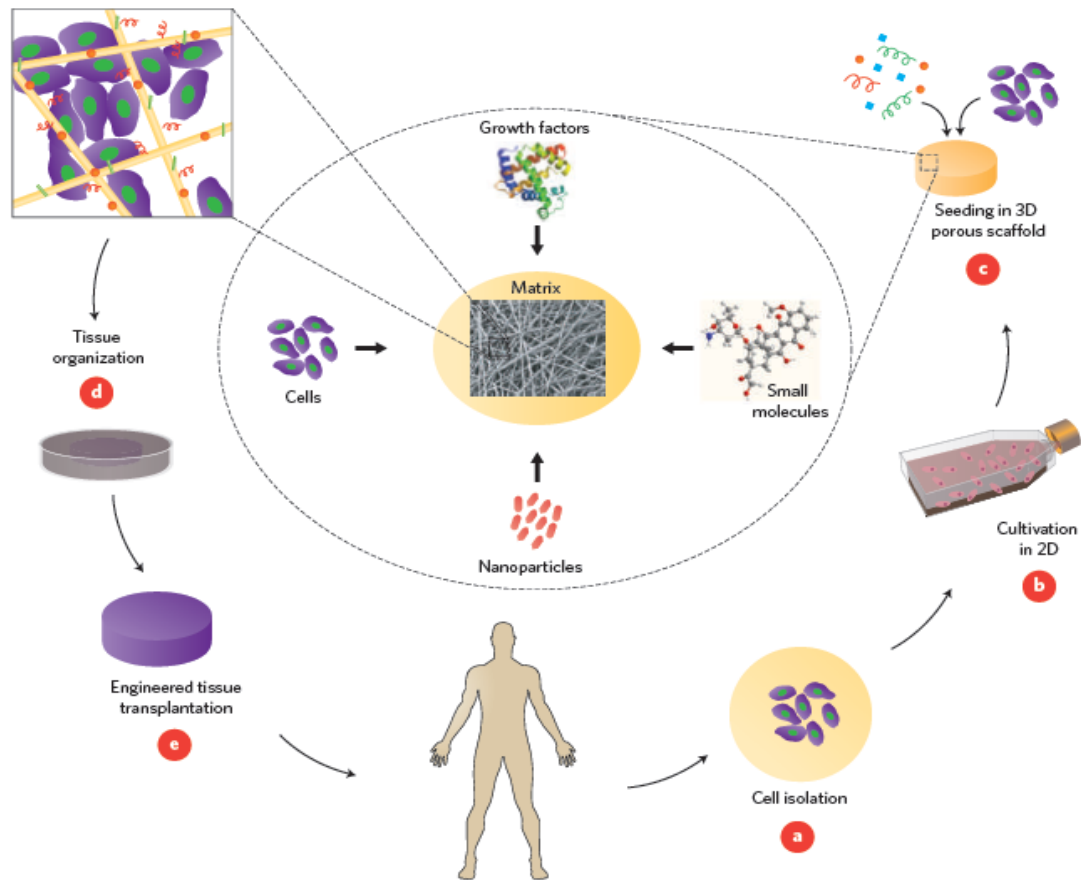


Fig. 2.1 – The Tissue Engineering Concept Map (T. Dvir, et al., 2011)

2.1.2 Bone

The development of biomaterials for bone tissue engineering requires physiological knowledge of the tissue matrix. This section covers the fundamentals of bone structure, development, and remodelling.

Structure

There are four types of bone: long bone, short bone, flat bone, and irregular bone (Jones, 2010; Stanfield & Germann, 2009). By weight, bone is composed of approximately 70% minerals (primarily hydroxyapatite), 22% proteins (primarily type I collagen), and 8% water (Shunji & et al., 2011). The structure of bone is depicted in Figure 2.2 below. The

inset shows a long bone, where the expanded sections at the end are referred to as the epiphysis, while the shaft is the diaphysis. The diaphysis is hollow and contains either two types of marrow. Red marrow is the site of blood production, and yellow marrow is comprised of adipose tissue (fat). A layer of periosteum covers the entire bone, except for its epiphysis where cartilage attaches and connects to tendons or ligaments. The bone's internal layer is referred to as spongy bone, which is also called cancellous or trabecular bone. Spongy bone contains a mesh-like network of trabeculae. Bone's external layer is called compact bone, also synonymous to cortical bone. Compact bone is organized into osteons (150-250 μm in diameter), each of which is centered around one to two blood vessels in the central or Haversian canal (25-50 μm in diameter). Perforating (Volkmann's) canals branch out at right angles of the central canal to connect to the periosteum's blood and nerve supply. The osteons layers around the central canal are called lamellae and in between them, the bone cells or osteocytes lie in the lacuna. Canaliculi, or small tunnels, connect the lacunae to each other and the lacunae's inner ring to the central canal. (Jones, 2010; Kulin, Jiang, & Vecchio, 2011; Professionals, 2008; Stanfield & Germann, 2009).

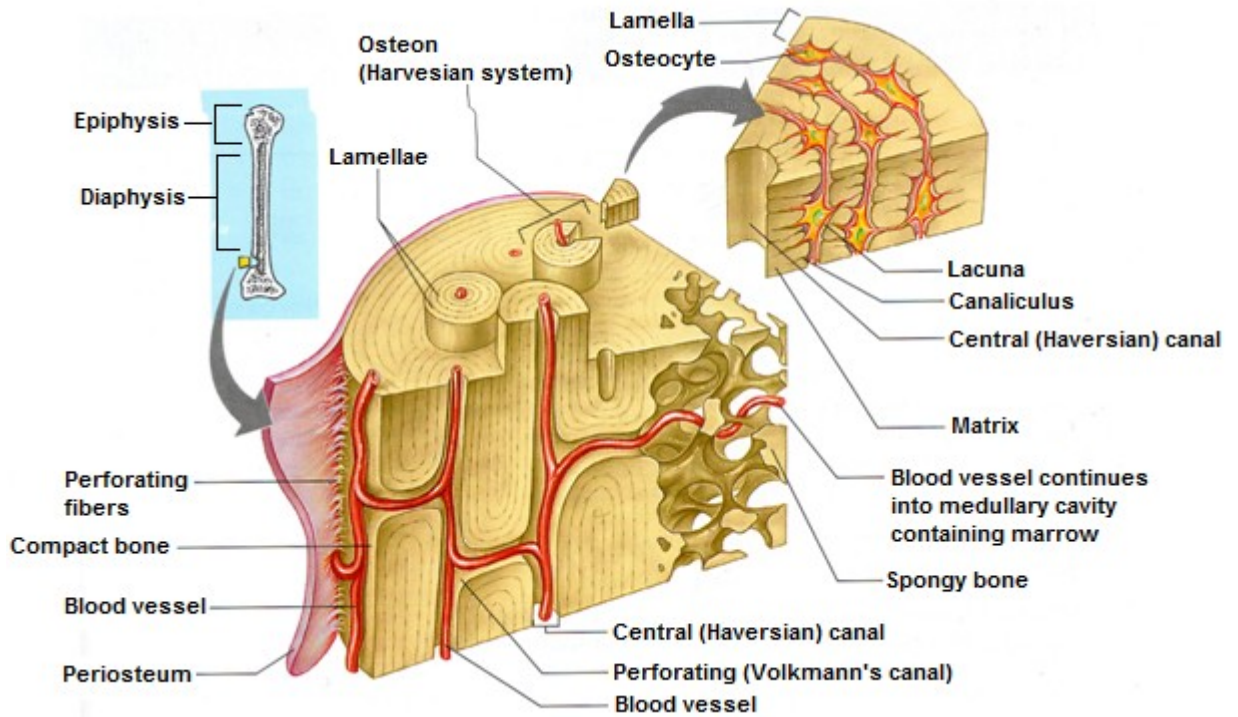


Fig. 2.2 – Bone (Jones, 2010; Professionals, 2008; Stanfield & Germann, 2009)

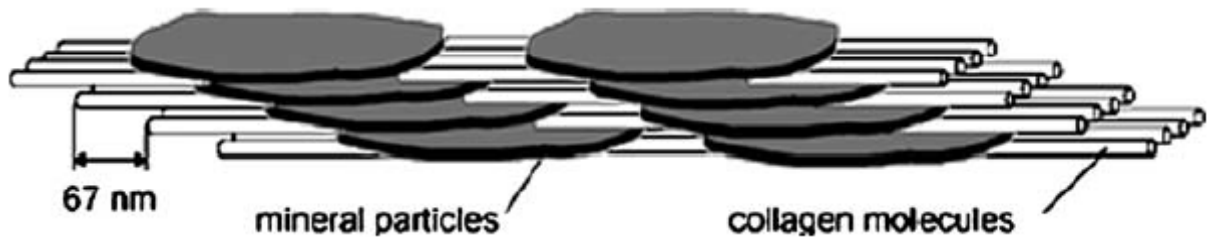


Fig. 2.3 – Collagen fibrils and minerals crystals arrangement in bone (Ruppel, Miller, & Burr, 2008)

Figure 2.3 depicts collagen fibrils and minerals crystals arrangement in bone, which make up its extracellular matrix along with other components such as laminin, fibronectin and vitronectin. Most collagen in bone tissue is tightly packed Type I collagen. Collagen fibrils are arranged rectilinearly with diameters in the range of 30-80 nm. Carbonated hydroxyapatite crystals are positioned in the gap-zones of the collagen fibrils and possess

a plate-like organization. These mineralites have a thickness less than 10 nm (Ruppel, et al., 2008).

Because apatite needles, collagen fibers, lamellae, Haversian systems, and blood vessels, all align and orient along the length of the bone, its tensile strength and stiffness are greater in the longitudinal direction (Wainwright, 1982). Cortical bone's modulus is 17.7 GPa and 12.8 GPa in the longitudinal and transverse directions, respectively. The modulus of cancellous bone is 0.4 GPa. Furthermore, the tensile strength of cortical bone is 133 MPa in the longitudinal, while 52 MPa in the transverse directions. On the other hand, the tensile strength of cancellous bone is 7.4 MPa (Tabrizian, 2011).

Development

The two developmental types of bone are intramembraneous ossification, and endochondral ossification. During intramembraneous ossification, a membrane like layer of connective tissue forms, which is then subject to invasion by blood vessels. The next step involves differentiation of osteoblasts that begin to deposit a bony matrix around them. This process results in the production of spongy bone along the blood vessels. As the space is filled, the outer layers become compact bone. The skull, jaw and collar bone are all examples of bone development via intramembraneous ossification. In endochondral ossification, bone begins as cartilage, which grows rapidly. The cartilage cells at the center then enlarge such that they destroy the nearby matrix. Subsequently, chondrocytes die and the matrix starts to calcify. At this stage, the periosteum forms around bone and blood vessels begin to invade. Some of the invading cells become osteoblasts and these form spongy bone. Concurrently, osteoclasts break down spongy

bone to form marrow. As osteoblasts continue to turn cartilage into bone, chondrocytes maintain new cartilage production, which results in bone growth. At puberty, a secondary ossification site forms in the epiphysis with the invasion of blood vessels. When osteoblasts make bone faster than chondrocytes produce cartilage, bone growth stops. The appearance of the epiphyseal line then denotes the end of epiphyseal growth. Figure 2.4 depicts bone development in endochondral ossification (Jones, 2010; Stanfield & Germann, 2009).

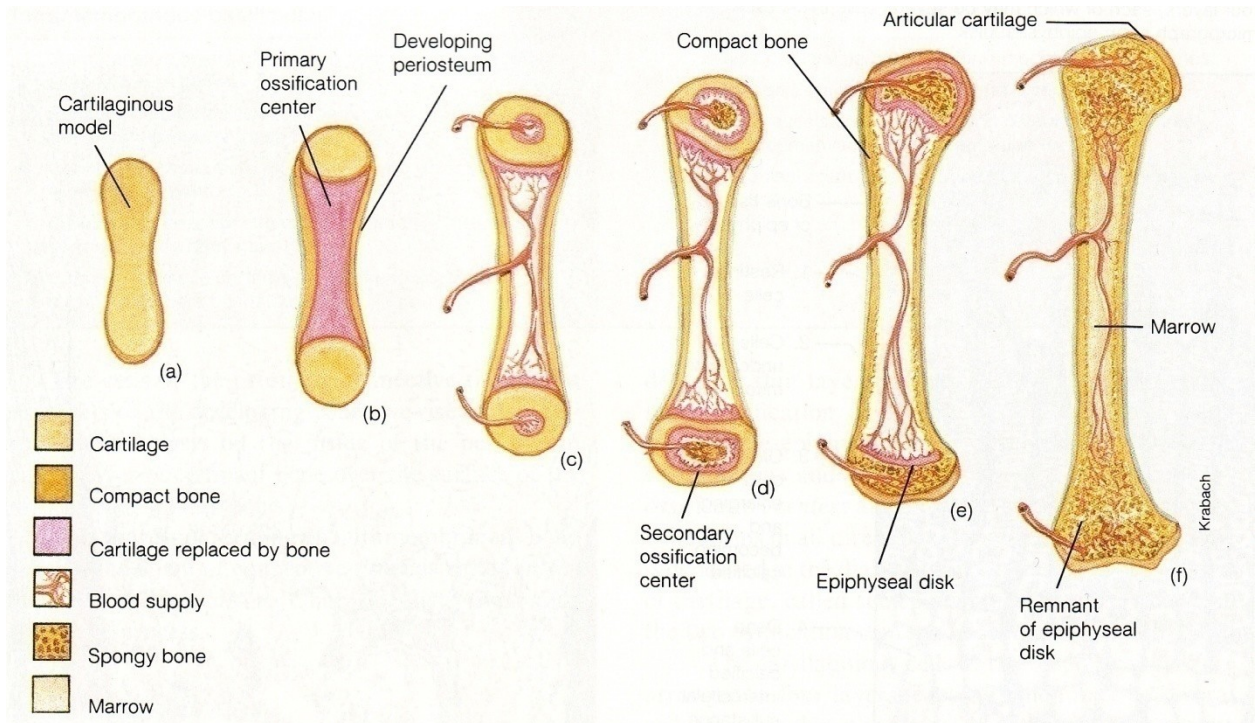


Fig. 2.4 – Bone development: endochondral ossification (Jones, 2010; Stanfield & Germann, 2009)

Remodelling

Bone is dynamic throughout life and remodels continuously because of changes in blood calcium levels as well as the pull of gravity and muscles. When blood calcium levels are

below homeostatic level, the parathyroid gland releases the parathyroid hormone, which leads to the activation of osteoclasts that break down the bone matrix. When bone is needed, osteoblasts lay down new matrix, become trapped and then differentiate into osteocytes. The pull of gravity and muscles determines where bone is remade. Wolff's Law summarizes the response of bone to mechanical load in stating bone adapts to the load it is placed under, in particular to the magnitude and direction of the applied force. Following the formation of the epiphyseal line, bone no longer grows in the longitudinal axis, but continues growing radially in response to forces (Jones, 2010; Lucas, Cooke, & Friis, 1998; Stanfield & Germann, 2009).

2.1.3 Characteristics of Scaffolds in Bone Tissue Engineering

An ideal scaffold for bone tissue engineering is one that mimics the extracellular matrix of the bone tissue it replaces (Shunji & et al., 2011). The three-dimensional scaffold must therefore have characteristics in line with those of bone. Some of the most essential properties for an ideal scaffold are outlined in Table 2.1.

Table 2.1 – Characteristics of the ideal scaffold

Property	Characteristics
Pores	Open & interconnected with porosity ~90 % & pore size larger than 100 μm (Burdick, Mauck, & SpringerLink (Online service), 2011; Karageorgiou & Kaplan, 2005; Salerno, Di Maio, Iannace, & Netti, 2011)
Mechanical integrity	Match trabecular bone native tissue stiffness ranging from 10 to 1500 MPa (Qin, 2007)
Bioactivity	Bonds to host tissue (Vadgama, 2005)
Biocompatibility	Does not result in formation of scar tissue (Vadgama, 2005)
Biodegradability	Resorbs at the same rate as tissue repairs, without generation of toxic by-products (Vadgama, 2005)
Osteoinductivity	Promotes bone tissue growth (Bulstrode, 2010)

Firstly, the scaffold must have a porous structure allowing transfer of oxygen and propagation of nutrients to the cells. Porosity, pore interconnectivity and pore size must be controlled to obtain a scaffold with a large surface area to volume ratio, which accommodates cell in-growth, and promotes vascularization (Burdick, et al., 2011). Trabecular bone has a typical porosity in the range of 50-90 % (Karageorgiou & Kaplan, 2005). While porous, the scaffold must sustain the equilibrium of the bone defect, and handle the mechanical load of the original tissue (Qin, 2007). The presence of a foreign structure in the body should not trigger a significant inflammatory response that can result in the formation of scar tissue, and the rejection of the implant. Therefore, the scaffold must be biocompatible (Anderson & Shive, 1997; Vadgama, 2005). Furthermore, to integrate with the surrounding tissue, the scaffold must be bioactive, which means form bonds with the bone matrix. Biodegradability is also an essential property sought in a scaffold since it is not intended to permanently replace bone, but only temporarily manage its function while the tissue gradually revives. Thus, the scaffold structure must gradually degrade to allow space for new tissue growth. This degradation must result in non-toxic by-products that can be easily excreted by the body (Vadgama, 2005). Since the scaffold surface is the first point of contact with the surrounding tissue matrix, its topographical and chemical features must promote cell adhesion, in other words, the scaffold should be osteoinductive and encourage bone tissue growth (Bulstrode, 2010; Hutmacher, 2000; Vadgama, 2005). Finally, additional desirable criteria for an ideal bone scaffold include the ability to be commercially producible and sterilized for a safe and effective delivery to the patient (Vadgama, 2005).

2.1.4 Scaffold Materials

for Bone Tissue Engineering

A wide array of biomaterials exists for use as scaffold material. This section discusses the most widely used biomaterials for bone tissue engineering.

Natural polymers

Natural polymeric materials have excellent biocompatibility. Furthermore, they often contain bio-functional molecules that serve as an intrinsic template for cell attachment and growth (Narayan, 2009; Sabir, Xu, & Li, 2009). The two main types of natural polymers for biomedical applications are polysaccharides and polypeptides. Polypeptides are a chain of amino acids linked by a peptide bond whereas polysaccharides are a chain of sugar units attached by a glycosidic bond. Collagen is an example of the former while chitosan of the latter. Although there is a variety of other natural polymers, more information about the two is provided below for illustration (Narayan, 2009).

Collagen

Collagen constitutes most of the organic part of bone (Shunji & et al., 2011). In terms of tissue regeneration, it is most widely applied for repair of soft tissue. Collagen enables cellular recognition and promotes cell adhesion. This natural polymer undergoes enzymatic degradation by metalloproteinases and collagenases, resulting in corresponding amino acids such as glycine and proline. Because of their high biocompatibility and porous structure, collagen sponges have been extensively studied as scaffold material for tissue engineering. However, although collagen can be processed into various forms such

as sheets, tubes, sponge's foams, fibrous powders, and dispersions, its variable physical, chemical, and degradation properties, as well as risk of infection is a concern (Sabir, et al., 2009).

Chitosan

Chitosan is normally extracted from the exoskeleton of crustaceans (Narayan, 2009). This polymer is derived from chitin, which is a cellulose-like polymer with unbranched chains of N-acetyl-D-glycosamine (Narayan, 2009; Sabir, et al., 2009). Therefore, chitosan is a polysaccharide consisting of β (1-4) linked D-glucosamine with randomly located N-acetylglucosamine groups (Sabir, et al., 2009). Chitosan has been studied as scaffold material. Its structurally defined matrix has been shown to support the attachment and expression of extracellular matrix components by chondrocytes (Narayan, 2009). Additionally, a sponge form of chitosan has been demonstrated to promote bone formation by rat osteoblasts (Seol et al., 2004).

Synthetic polymers

Synthetic polymers are the most commonly used materials for bone tissue engineering. Unlike natural polymers, they are synthesized with a predictable lot to lot uniformity, and thus do not raise immunogenicity concerns. Synthetic polymers are also a reliable source of raw material (Sabir, et al., 2009). The most widely used synthetic biopolymers, both poly- α -hydroxy-esters, are polylactic acid (PLA) and polyglycolic acid (PGA) (Santin, 2008). Because of their proven biocompatibility and biodegradability, PLA and PGA are approved by the U.S. Food and Drug Administration (FDA) for many medical applications (Herren, Nagy, Campbell, & Federation of European Societies for Surgery of

the Hand. Meeting, 2008). These polymers degrade through a hydrolysis reaction, without any enzymes, which breaks them down to natural, non-toxic metabolites such as lactic acid, glycolic acid, water and carbon dioxide (Santin, 2008). The properties of PLA, PGA, and their copolymers are shown in Table 2.2. Others synthetic polymers, such as poly(ϵ -caprolactone) or poly(methyl methacrylate), are also commonly used in biomedical applications (B. Stevens, Yang, MohandaS, Stucker, & Nguyen, 2008).

Table 2.2 – Properties of synthetic biodegradable polymers (Santin, 2008)

Polymer	Melting point ($^{\circ}$ C)	Glass transition temperature ($^{\circ}$ C)	Degradation time (months) ^a	Tensile strength (MPa)	Elongation (%)	Modulus (GPa)
PGA	225-230	35-40	6-12	>68.9	15-20	6.9
PLLA	173-178	60-65	>24	55.2-82.7	5-10	2.8-4.2
PDLLA	Amorphous	55-60	12-16	27.6-41.4	3-10	1.4-2.8
PLGA	Amorphous	45-55	0.8-10	41.4-55.2	3-10	1.4-2.8
PCL	58-63	65	>24	20.7-34.5	300-500	0.21-0.34

^aTime to complete mass loss. Rate also depends on part geometry

Poly(lactic acid (PLA)

The ring opening of lactide yields poly(lactic acid (PLA) (Hollinger, 2005). Figure 2.5 shows the chemical pathway for PLA synthesis (Santin, 2008). Lactic acid is a chiral molecule and, as a consequence, PLA has three different isomeric forms. Poly-L-Lactic Acid results in poly(L-lactide) or PLLA, Poly-D-Lactic Acid results in poly(D-lactide) or PDLA, and finally Poly-D,L-Lactic Acid results in poly(DL-lactide) or PDLLA (Santin, 2008). Processing conditions and properties of PLAs are strongly dependent on whether they have a crystalline or amorphous structure (Auras, 2010).

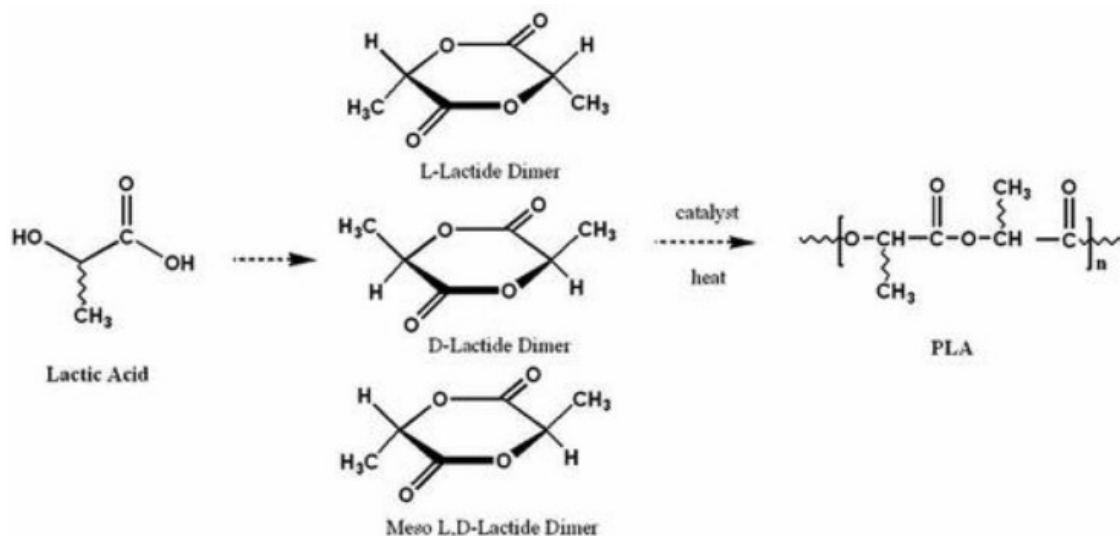


Fig. 2.5 – Synthetic pathway for PLA synthesis (Santin, 2008)

Polyglycolic acid (PGA)

The ring opening of glycolide yields polyglycolic acid (PGA) (Hollinger, 2005). Figure 2.6 shows the synthetic pathway for PGA synthesis (Santin, 2008). PGA is only soluble in very few, quite toxic solvents such as hexafluoroisopropanol. As a consequence, PGA is mostly used as a copolymer with PLA (Hollinger, 2005).

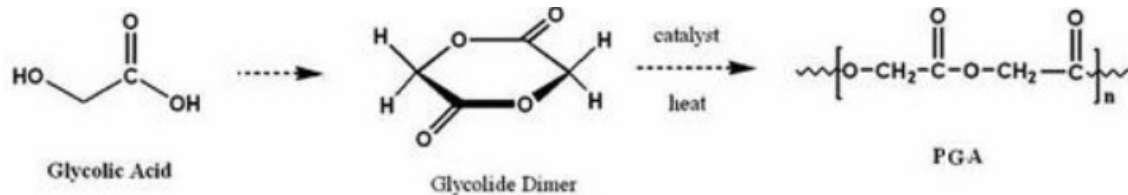


Fig. 2.6 – Synthetic pathway for PGA synthesis (Santin, 2008)

The chemical steps to obtain PGA and PLA are shown in Fig. 2.7. The process first starts with glycolic (to get PGA) or lactic (to get PLA) acids that go through a condensation reaction to yield low molecular weight polymers. A thermal treatment of the latter gives

glycolide (for PGA) or lactide (for PLA), which are cyclic dimeric units. Afterwards, these undergo purification and are polymerized by ring opening that leads to the high molecular weight polymers, PGA or PLA (Santin, 2008):

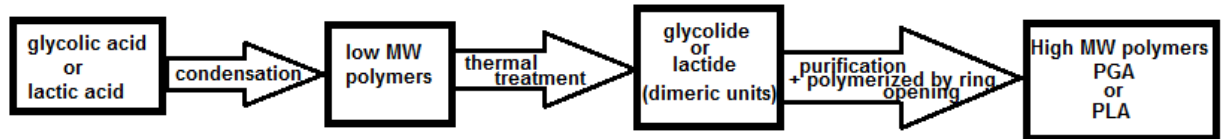


Fig. 2.7 – Chemical steps to PGA or PLA (Santin, 2008)

Despite the fact that PGA and PLA have similar structures, the methyl group on the alpha carbon of PLA, Fig. 2.8, makes these two polymers very different in terms of their chemical, physical and mechanical properties. PGA is more hydrophilic and acidic, whereas PLA is hydrophobic and less acidic. As a consequence, their degradation rate in fluids and bi-response differs (Santin, 2008).

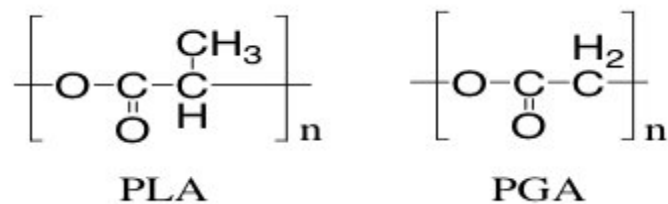


Fig. 2.8 – PLA and PGA structures (Ratner, 2004; Wnek & Bowlin, 2004)

Poly-D-Lactic acid (PDLLA) & Poly-L-Lactide Acid (PLLA)

Both L- and D- lactic acid stereoisomers are found in nature, but the most common is the L- type and the racemic mixture of L- and D-lactides or simply PDLLA. The lactic acid produced in the human body is the L-enantiomeric form and the D-isomer is not subject

to much investigation. Biomedical research thus mostly involves PLLA and PDLLA, while PDLA has some applications in medicinal chemicals (Auras, 2010).

PLLA is a semicrystalline polymer because of the enantiomeric purity of the pristine monomers and the stereoregularity of the polymer chain (Albertsson, 2002). Crystalline polymers degrade slower (Barbucci, 2002). Therefore, since PLLA is semicrystalline while PDLLA is completely amorphous because of its irregular structure, PLLA degrades slower than PDLLA (Fig. 2.9) (Chu & Liu, 2008). In any case, the degradation product of both PLLA and PDLLA is lactic acid (Fig. 2.10) (Atala, 2010).

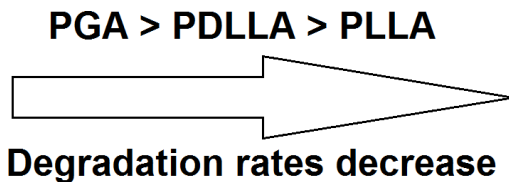


Fig. 2.9 – Degradation Rates of Biomedical Polyesters (Chu & Liu, 2008)

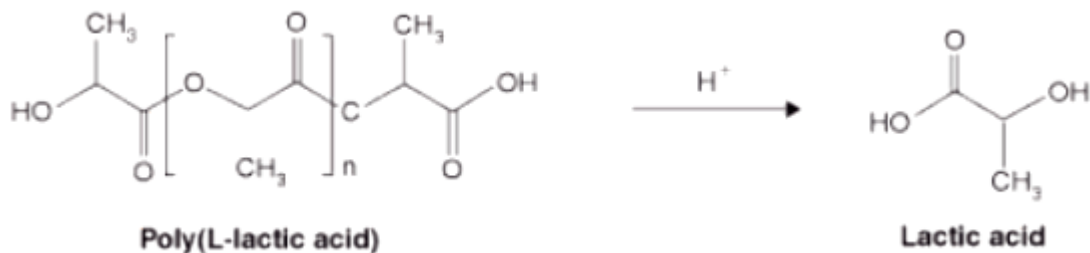


Fig. 2.10 – Degradation Product of PLLA (Atala, 2010)

Poly(lactic-co-glycolic) acid (PLGA)

As its name suggests, poly(lactic-co-glycolic) acid is the copolymer of PLA and PGA, and has been under extensive investigation for tissue engineering applications. The synthetic pathway of PLGA is shown in Figure 2.11.

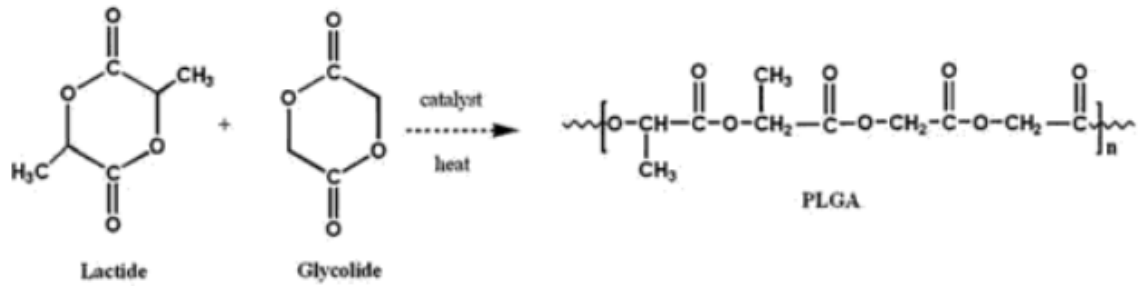


Fig. 2.11 – PLGA Synthesis (Santin, 2008)

PLGA copolymer with 82% PLLA and 18% PGA is commercially sold under the product name LactoSorb, and it has been clinically used in craniofacial reconstruction for six years (Hollinger, 2005). Experimental *in vivo* and *in vitro* studies show that PLGA degrades in 3-4 weeks while polylactic acids lasts much longer, even 3-4 years (Barbucci, 2002). PLGA degrades into both lactic and glycolic acids that are non-toxic (Fig. 2.12).

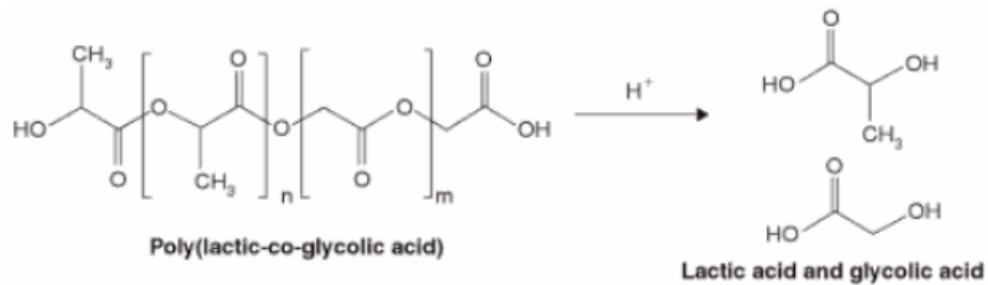


Fig. 2.12 - Degradation Product of PLGA (Atala, 2010)

Bioceramics

Bioactive ceramics are biomaterials that have the ability to form a biological bond with bone tissue, which makes them ideal candidates for scaffolding materials for bone tissue engineering (Ducheyne & Qiu, 1999; Hollinger, 2005; Ma & Elisseff, 2005).

Bioglass 45S5

Bioglass 45S5 is a melt-derived, commercially available, bioactive glass with 45% SiO₂, 24.5% Na₂O, 24.5% CaO, 6% P₂O₅ weight percent set composition. Currently, BG is used in the medical field as bone and tooth regenerative material and classified as class A bioactive material. It is biodegradable, biocompatible, and approved by the FDA for use in the body. When in contact with body fluids, BG dissolves and generates silicate, phosphate, calcium and sodium ions. Calcium and phosphate ions reprecipitate on the BG surface and form a layer of hydroxyapatite [Ca₁₀(PO₄)₆(OH)₂ + CO₃²⁻] similar to the mineral found in bone. This apatite layer later integrates with the surrounding tissue fibrillar collagen, and forms a matrix that attracts osteoblasts and incites bone tissue regrowth. For the purposes of bone tissue engineering, BG leads nucleation and growth of a HA layer on the scaffold surface. Therefore, the artificial matrix can better integrate with the surround tissue matrix and develops enhanced osteoconductivity (Boccaccini & Maquet, 2003). The stages of reactivity of BG when in body fluid, which ultimately lead to the formation of a hydroxycarbonate apatite layer, have been proposed by L.L. Hench and summarized in Figure 2.13:

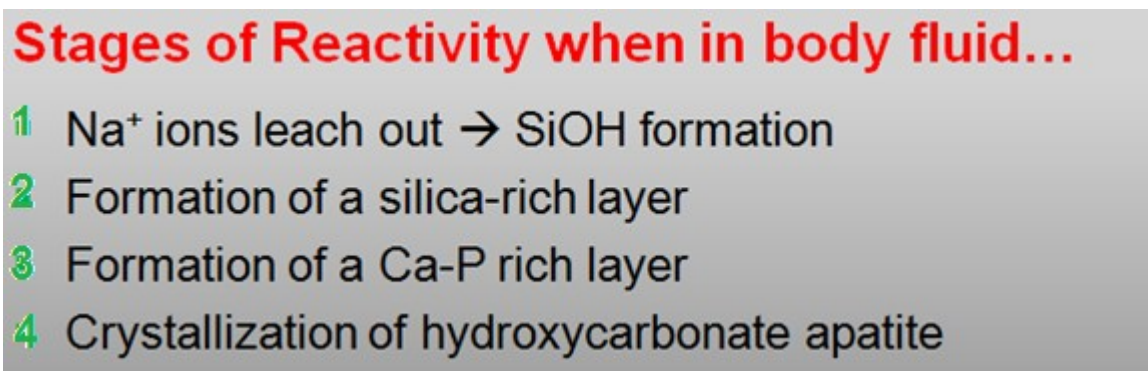


Fig. 2.13 – Stages of Bioglass 45S5 reactivity (Boccaccini & Maquet, 2003)

Bioglass is comprised of the four main elements of Si, Ca, Na, and P. When in body fluid, the first thing that happens is Na ions leach out of the glass and the hydrogen ions in solution form ionic bonds with the surface, leading to SiOH formation. Subsequently, a silica rich layer is formed on the surface, which facilitates the diffusion of the two other elements, Ca and P, from the bulk to the surface of the glass. Thus, in the third step, we have formation of a Ca-P rich layer that then crystallizes to form the layer of hydroxycarbonate apatite (Hench, 1977; Hench, et al., 1973).

Composites

A major scaffold design problem is the selection of an appropriate material that meets all necessary bone scaffold characteristics outlined in Table 2.1. In fact, no such single material exists, and composite scaffolds are a promising option mimicking the bone's natural inorganic-organic structural mixture. A composite material is comprised of two or more materials (Sabir, et al., 2009). A composite scaffold can for instance consist of a polymer that provides toughness along with an inorganic, bioceramic material that makes it bioactive and improves scaffold mechanical properties (B. Stevens, et al., 2008). Examples of such composite systems are Tricalcium phosphate-collagen, HA-PLGA, or BG-PLLA, which studies have shown to act as promising scaffolds for bone regeneration (Hollinger, 2005; B. Stevens, et al., 2008).

2.1.5 Scaffold Fabrication Techniques

Several scaffold preparation techniques exist, and some of the most common ones for bone tissue engineering are described in this section.

Solvent casting & particulate leaching

Solvent casting and particulate leaching was first introduced by Mikos et al. in 1994 and used for the preparation of poly(L-lactic acid) foams as scaffolds (Mikos et al., 1994). This technique involves dissolving the scaffold material in an organic solvent and adding a water soluble porogen such as salt to the mixture, which is then mould casted. Once the solution solidifies and the solvent is evaporated, the structure is then immersed in water until the porogen is completely dissolved, leaving a porous polymeric scaffold. Disadvantages of the technique include the potential presence of porogen residuals in the scaffold and recourse to toxic organic solvent for dissolving the polymer. Nevertheless, this is one of the original and simplest techniques for scaffold fabrication that is still in used today, a decade after it was first introduced (Hollinger, 2005).

Phase separation

Thermally induced phase separation (TIPS) involves decreasing the temperature of a polymer solution to induce the separation of two phases, one rich in polymer and the other having a low polymer concentration. The solvent in the polymer-lean phase is then removed by evaporation, sublimation, or extraction, leaving behind open pores in solidified polymer foam. Advantages of this technique include the ability to partially control the micro and macrostructure of the polymer foam by varying the phase separation temperature among other parameters. However, using this technique can be a complicated process because it depends on the thermodynamic and kinetic behaviour of the polymer solution at given conditions (Ma & Elisseeff, 2005). A disadvantage is also the use of toxic organic solvent.

Gas foaming

In gas foaming, solid pieces of polymers are exposed to and saturated with high pressure (800 psi) carbon dioxide gas. When the pressure is slowly reduced to atmospheric, carbon dioxide nucleates and grows within the polymer, resulting in pore formation. This technique is advantageous because it does not require toxic organic solvents. However, a disadvantage is that not all pores are interconnected (Hollinger, 2005; Meyer-Blaser, Handschel, Meyer, Wiesmann, & SpringerLink (Online service), 2009).

Three-dimensional printing

3D printing is one of many solid free form fabrication (rapid prototyping) techniques, all of which involve manufacturing scaffolds in a layer by layer fashion from the three-dimensional computer design of the object (Ma & Elisseeff, 2005). The main advantage of 3D printing is that scaffolds are made at room temperature, thereby allowing cell seeding or incorporation of growth factors during fabrication (Meyer-Blaser, et al., 2009). In 3D printing, a solvent is directed into a polymer powder packed with salt particles and a complex three-dimensional structure is built by laying down a series of very thin, two-dimensional slices. The salt particles are then dissolved through immersion of the polymer/salt composite in water, resulting in a porous scaffold (Hollinger, 2005). Concerns regarding this technique are residual remains of toxic organic solvents (Ma & Elisseeff, 2005).

2.2 Molding Material

This section gives an overview of candidate materials that either have the potential applicability or are currently used in biomedical applications, specifically for molding. The typical material used in the solvent casting and particulate leaching technique for scaffold mold is Teflon (Liao et al., 2002; Mikos, et al., 1994; Suh et al., 2002). Thus, the materials under investigation in this segment include Teflon, as well as Sil940, polyurethane, polyether, and polydimethylsiloxane (PDMS). Reasons for their selection as well as some of their relevant characteristics are the subject of the review herein.

2.2.1 Teflon

A fluorocarbon-based polymer, Teflon, was discovered in 1973 by Dr. Roy J. Plunkett. It is manufactured only by DuPont and widely used for its chemical resistance, low and high temperature capability, resistance to weathering, low friction, electrical and thermal insulation (Hougham, 1999). The material has many applications in bioengineering. For instance, Dacron or polytetrafluoroethylene (PTFE) is utilized for prostheses of blood vessels (Xue & Greisler, 2003). Boccafoschi and colleagues (Boccafoschi, Habermehl, Vesentini, & Mantovani, 2005) investigated the impact of collagen when in contact with blood and cells to assess its suitability as scaffold materials for vascular tissue engineering. In this study, Teflon was used as a reference material for clotting time measurement and thromboelastography. On the other hand, glass was used as negative control because of its negative reaction when in contact with blood. The longer the clotting time, the better the compatibility between the substrate and blood, and thus the amount of free haemoglobin was measured for evaluating the potential of a substrate to

not induce immediate clotting. Results show that collagen is less efficient than Teflon in enhancing clot formation. (Fig. 2.14a). Thrombelastography test gives information about several steps in the coagulation process including the time required for fibrin formation, and there is no significant difference in fibrin formation time between collagen and Teflon (Fig. 2.14b). Thirdly, the thrombogenicity index, which is an indication of the dynamics of blood coagulation as well as the strength of the final clot, displays a similar trend for both Teflon and collagen. Platelets and fibrin weakly interact in blood after contact with both substrates (Fig. 2.14c). Generally, this investigation attests the bio-applicability of Teflon as its biological performance is compared step by step with collagen, and although centered on the latter, equally proves the potential for the former as scaffold materials for vascular tissue engineering.

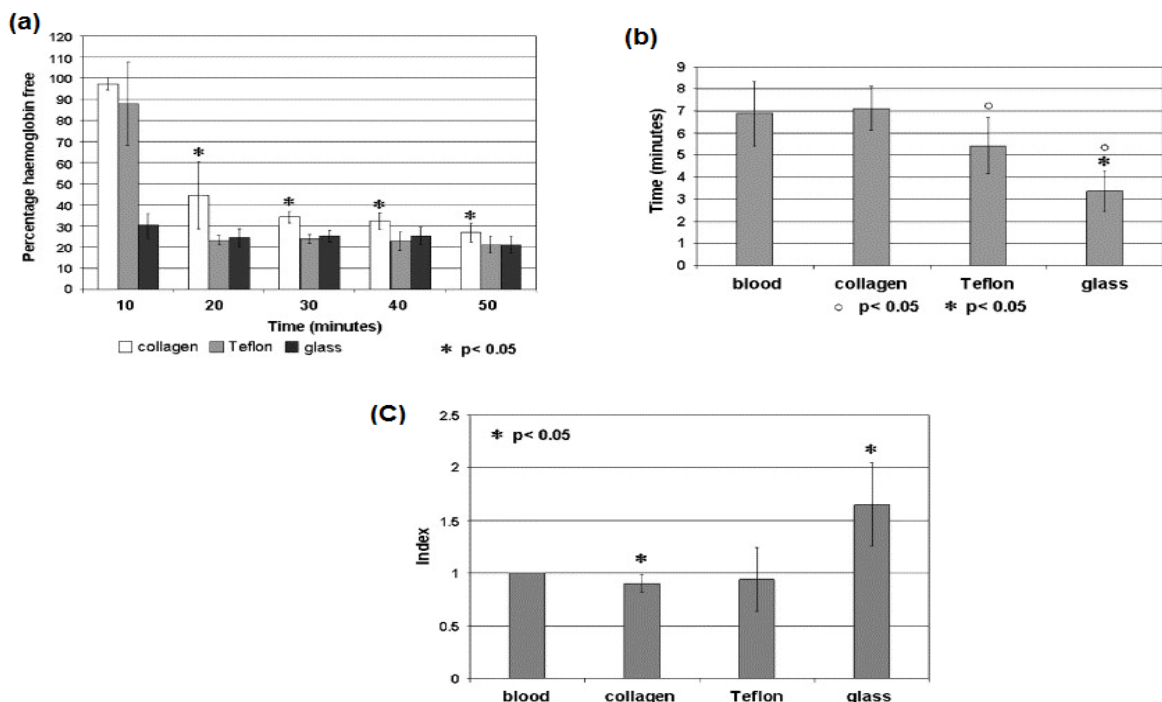


Fig. 2.14 – Haemoglobin free test on collagen, Teflon and glass (a); fibrin formation (b); thrombogenicity index (c). * indicates that results are statically significant (Boccafoschi, et al., 2005)

Teflon is also widely applied in constructing molds for scaffold fabrication, especially in the solvent casting and particulate leaching technique, where it is used to cast a polymeric paste (Lanza, Langer, & Vacanti, 2007). The Teflon for molding must provide a solid framework to shape the scaffold. It is thus not the same grade type of flexible Teflon employed for vascular grafts. Molding Teflon, although also inert, is rigid and requires machining to obtain the desired shape (Chatterjee et al., 2010; Loh, Chester, & Taylor, 1993).

2.2.2 Sil940

Silicone-based molds have been used in biomedical applications such as casting a poly(propylene fumarate) for implant fabrication (Guelcher & Hollinger, 2006). Sil940 is a molding material commercialized by Smooth-On, Inc. This platinum cure silicone, also referred as “addition cure silicone”, is high tear strength, flexible, two component mold compound. Silicone molds prepared with Sil940, exhibit very low shrinkage and high physical properties. Therefore, although recommended for casting polyurethane, epoxy, and polyester resins, and wax, mold made from Sil940 can be potentially suitable candidates for molding polymeric pastes. Sil940 in particular is suitable to make food grade materials, and complies with the total rubber extractive limits as specified and published by the FDA. These rubbers can also be used to cast prosthetics for special effects makeup and medical purposes (Smooth-On, 2011b).

2.2.3 Polyurethane

Polyurethane can be used to generate flexible material and can thus be a potential candidate material for mold design applications of scaffolds. There are a wide range of

polyurethane materials with different grades and flexibility. The polyurethane investigated in this study is from Smooth-On, Inc., the ReoFlex series. Even within the same series, there is a possibility for tailoring the material’s hardness. Table 2.3 demonstrates the properties of different grade polyurethane rubbers in this series (Smooth-On, 2011a).

Table 2.3 – ReoFlex® Urethane Rubber Properties

Product Name:	A:B Mix Ratio	Demold Time	Elongation at Break	Mixed Viscosity	Pot Life	Shore A Hardness	Tear Strength	Weight: CU.IN./LB
ReoFlex® 20	1:1 by volume	16 hours	1000%	1500 cps	30 min.	20	60 pli	27.3
ReoFlex® 30	1:1 by volume	16 hours	1000%	1800 cps	30 min.	30	82 pli	27.5
ReoFlex® 40	1:1 by volume	16 hours	1000%	1500 cps	30 min.	40	85 pli	27.2
ReoFlex® 50	1:1 by volume	16 hours	432%	2000 cps	50 min.	50	120 pli	27.4
ReoFlex® 60	1:1 by volume	16 hours	581%	1800 cps	50 min.	60	132 pli	26.7

2.2.4 Polyether

Polyether based materials are hydrophilic and used clinically to create teeth impressions in dentistry. Given its flexibility and proven safe usage in the body, the “Impregum Penta Soft Medium Body” by 3M is thus investigated in this study as potential mold material for scaffold fabrication. A peculiarity with polyether is its “snap-set” behaviour as a result of which it does not start setting before the working time ends, yet setting occurs immediately (Fig. 2.15) (ESPE, 2011).

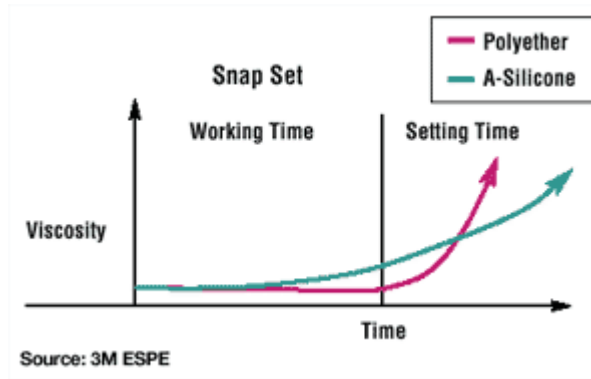


Fig. 2.15 – Snap-Set Time: Polyether vs. Silicone (ESPE, 2011)

2.2.5 Polydimethylsiloxane (PDMS)

PDMS is a silicone elastomer traditionally used as a biomaterial in catheters and other biomaterials. It is transparent, non-fluorescent, biocompatible and nontoxic. Recently, PDMS gained wide popularity for the development of microelectromechanical systems (MEMS) and microfluidics components for biomedical applications. The use of PDMS in MEMS applications is driven by the development of Soft Lithography techniques such as micro-contact printing, which uses PDMS to create an elastomeric stamp that incorporates microstructures for transfer of patterns onto a subsequent substrate. This material has a lower cost than silicone, in addition to being chemically inert, thermally stable, permeable to gases, simple to handle (Mata, Fleischman, & Roy, 2005). There has thus far been no mention of PDMS use as molding material during the solvent casting/particulate leaching technique. Since the material is flexible with proven applicability in many area of biomedical engineering, its use will be investigated in this study for making scaffolds.

3 – Methodology

The methodology outlines the materials and methods of this study. It is comprised of two parts. The first focuses on the steps involved in composite PDLLA-Bioglass scaffold preparation and analysis, while the second deals with mold design and characterization.

3.1 Materials

Materials for Scaffold Synthesis

PDLLA “RESOMER R 208” (MW=200,000) has been kindly provided by Boehringer Ingelheim Chemicals, Inc. The porogen used is sodium Chloride (NaCl) reagent grade $\geq 98\%$, +80 mesh particle size, which is supplied from Sigma-Aldrich, Inc., along with acetone CHROMASOLV[®] Plus for HPLC $\geq 99.9\%$, and Silver Nitrate (AgNO₃) ACS reagent $\geq 99.0\%$. Bioglass 45S5 of two different sizes, A) 90-710 μm , and B) $< 120 \mu\text{m}$ has been kindly offered by NovaBone Products, LLC.

Materials for Molding

Teflon spray (MS122E, MS-122AD) was kindly provided by the Miller-Stephenson Chemical Company, Inc. Polydimethylsiloxane (PDMS) was also provided. Teflon blocks were purchased by the Department of Mining & Materials Engineering machine shop. The molding kit for Sil940 was purchased from Smooth-On, Inc. A sample of polyurethane substrate, ReoFlex series, was kindly provided from Smooth-On, Inc. The Rust-Oleum Specialty Lacquer was purchased from a hardware store. Finally, the molding material and equipment for polyether was kindly offered by Dr. Faleh Tamimi (Department of Dentistry, McGill University).

3.2 Composite

PDLLA-Bioglass Scaffolds

3.2.1 Characterizations

Particle Size Analysis

The two different size groups of Bioglass, A) $\leq 90 \mu\text{m}$, and B) $710 \mu\text{m}-90 \mu\text{m}$, are referred to as BGA and BGB, respectively. The average particle size of the two BG groups is determined using the Horiba Laser Scattering Particle Size Analyzer (size range from 0.020 to 2000 microns).

Inductively Coupled Plasma Optical Emission Spectroscopy (ICP-OES)

An elemental analysis of the aqueous solution in which BGA and BGB are immersed after only a two day water treatment period (Fig. 3.1a), and a two day acetone treatment followed by another two day water treatment (Fig. 3.1b) is conducted with an inductively coupled plasma optical emission Spectrometer, Perkin Elmer Aanalyst 100 AAS. The absorption wavelengths used to determine Ca, P, Si, and Na are shown below in Table 3.1.

Table 3.1 – ICP emission lines

Element	Lines of Emission
Si	251.611 nm
Ca	317.933 nm
Na	589.592 nm
P	213.617 nm

Standard solutions of 1, 10, and 100 ppm for Ca, Na, P, and Si are prepared. A “Blank” sample with just distilled water is also used as control. Three replicates were made for each element.

Fourier Transform Infrared Spectroscopy (FTIR)

FTIR is a surface sensitive technique used to analyze the chemical transformations occurring on the surface of both BG powdered samples, and solid polymeric scaffolds. FTIR analysis with a detection range of 1-5 μm depth, and 1 mol % analytical sensitivity was performed using the Bruker Tensor 27 IR spectrometer, equipped with both a DTGS and an MCT detector. Diffuse Reflectance Infrared Fourier Transform (DRIFT) spectroscopy has been applied, and spectra were recorded using Deuterated tri-glycine sulfate pyroelectric (DTGS) detector with 128 scans and 4 cm^{-1} resolution.

BG powder samples are mixed with KBr in a ratio of 1:4. Potassium bromide (KBr) is transparent to infrared light and therefore has no visible peaks. For FTIR spectroscopy, KBr is thus useful, particularly in two instances: 1) to measure the background, and 2) to dilute the sample. The scaffold surface is analyzed both before and after BG addition. Since the scaffold is a solid, the dilution with KBr was not possible and the 3D structure was simply placed on the sample holder for analysis.

pH Analysis

In the dissolution experiments, 10 mL DI water and 32 mg of BG (i.e. 0.32 % w/v) are combined and the effects of BG ionic release in the aqueous solution is monitored by measuring the pH of the stirred supernatant at regular intervals (every 0, 30, 90, 210, and 330 minutes for both BGA and BGB). For comparison purposes, BG ionic release

behaviour within the scaffold polymeric matrix was evaluated by measuring pH of the scaffolds immersed in DI water with the same BG mass-volume percentage (i.e. 0.32 % w/v), and at the same regular time intervals (every 0, 30, 90, 210, and 330 minutes) as in the BG dissolution experiments.

Scanning Electron Microscopy (SEM)

Scaffold morphology is assessed using the Phenom desktop electron microscope where samples are viewed without prior preparation.

X-Ray Photoelectron Spectroscopy (XPS)

Bioglass 45S5 after Extraction from Scaffold

XPS (ThermoFisher Scientific K-Alpha X-Ray Photoelectron Spectroscopy) spectroscopy with 10-100 Å depth, and 0.1 % analytical sensitivity is a more surface sensitive technique relative to FTIR. A spot size of 400 x 750 µm², and 1350 eV X-Ray energy (K_α Al emission) was employed for the analysis. The aliphatic C peak at 285 eV was used to calibrate the energy scale of spectra in the first part of this work; energy scales were not calibrated after collection of the spectra relative to the scaffold mold study. The surface of BG powder samples was analyzed for Ca, Na, P, and Si. To characterize PDLLA films cast on each different potential mold substrate material. Some of the materials were etched up to a depth of 15 nm using an Ar gun (Total of 3 levels, 5 s etching for each level, approximate etch rate for PDLLA=1 nm/s). In addition to an elemental survey and high resolution spectra for Si, C, O, and/or N were collected.

3.2.2 Bioglass 45S5 Preliminary Analysis

The overall objective of the study is to see how Bioglass changes in terms of structure and composition throughout the scaffold processing. However, the transformation of Bioglass must first be monitored independently of the scaffold's polymeric environment. Therefore, in this preliminary study, the behaviour of Bioglass within the different solutions involved in the scaffold processing is first analyzed. During the scaffold preparation, Bioglass is added to a polymer mixture of PDLA & acetone, and this mixture is then cast into a mould. The resulting scaffold is then immersed in water to leach out the salt porogen. Hence, Bioglass is first in contact with acetone and subsequently with water.

The preliminary study involves two different size groups of Bioglass, A) $\leq 90 \mu\text{m}$, and B) $710 \mu\text{m}-90 \mu\text{m}$. For each group, the average as received BG particle size is first determined through a particle size analysis, followed by an inspection of the BG surface chemical environment using FTIR spectroscopy, and an assessment of BG reactivity in dissolution experiments where pH is monitored. Subsequently, each different size BG is treated in acetone, the first solution involved in the scaffold processing. Physical and chemical effects of acetone on BG are then evaluated by comparing average particle size and FTIR spectra with the original as received BG (Fig. 3.1a).

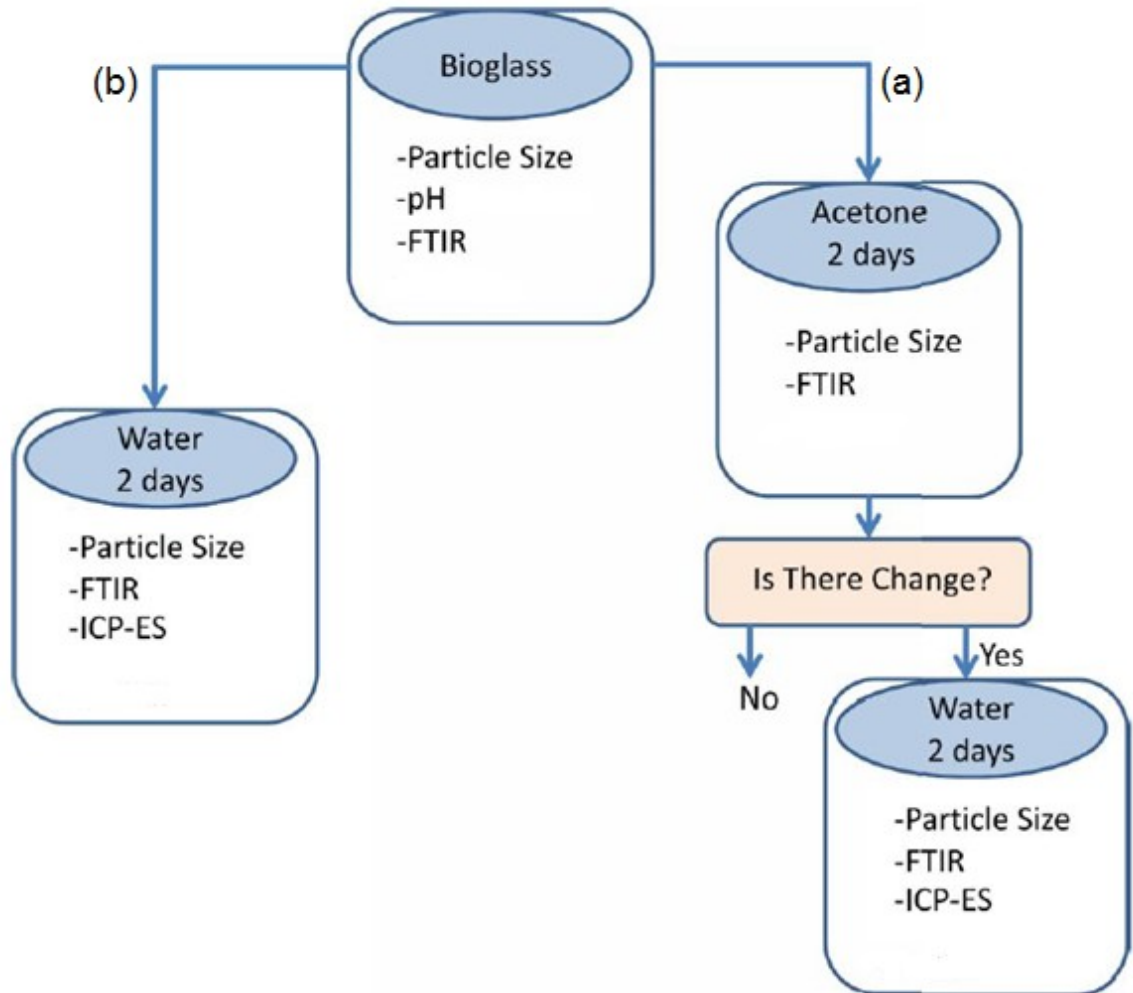


Fig. 3.1 – Preliminary Bioglass 45S5 Analysis Scheme

Subsequent to acetone treatment, BG groups are immersed in water, the second solution involved in scaffold preparation, for two days. This is the same time period that BG is exposed to water during the leaching step of scaffold processing. Possible changes in BG are detected via particle size analysis, and FTIR spectroscopy. ICP-OES is performed on the resulting solution to see whether the elemental release behaviour and stages of BG reactivity (Fig. 2.14) is the same after BG treatment in the scaffold’s processing solutions. To understand the sole effect of water on BG during the salt leaching step of scaffold preparation (see section 3.1.3 Scaffold Processing), the same characterization steps

(particle sizing, FTIR, ICP-OES) are conducted on BG after a two days water treatment period without prior contact with acetone (3.1b).

3.2.3 Scaffold Processing

Pore Size of Scaffold

The scaffold pore size depends on the size range of the select porogen. Sodium chloride (NaCl) with an average 80 mesh (180 μm) particle size is used as porogen. To obtain particles within the desired pore size range of 75 μm -355 μm , the salt is sieved using two sieves possessing the upper and lower size limits (Fig. 3.2).

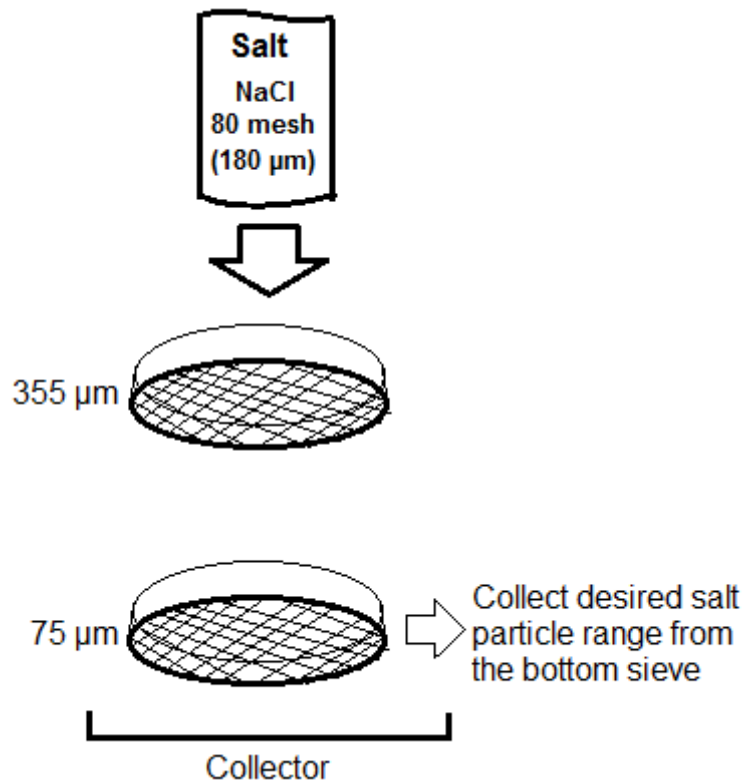


Fig. 3.2 – Porogen Range for Scaffold Pore Size

The Silver Nitrate Test

The silver nitrate test is performed in order to make sure no salt residue remains after the water leaching step of scaffold processing. Upon silver nitrate addition, if Cl^- ions are still present due to the NaCl , then a white precipitate will be seen because AgCl will form. If no white precipitate is seen, then all salt has leached out (Magno et al., 2010). A silver nitrate (AgNO_3) 2.5 % (w/v) solution is made by adding 2.5 g of AgNO_3 to a 100 mL flask.

Scaffold Preparation

The solvent casting and particulate leaching technique is used to make the composite scaffolds (Fig. 3.3). The process is described in detail by Mikos and colleagues (Mikos, et al., 1994).

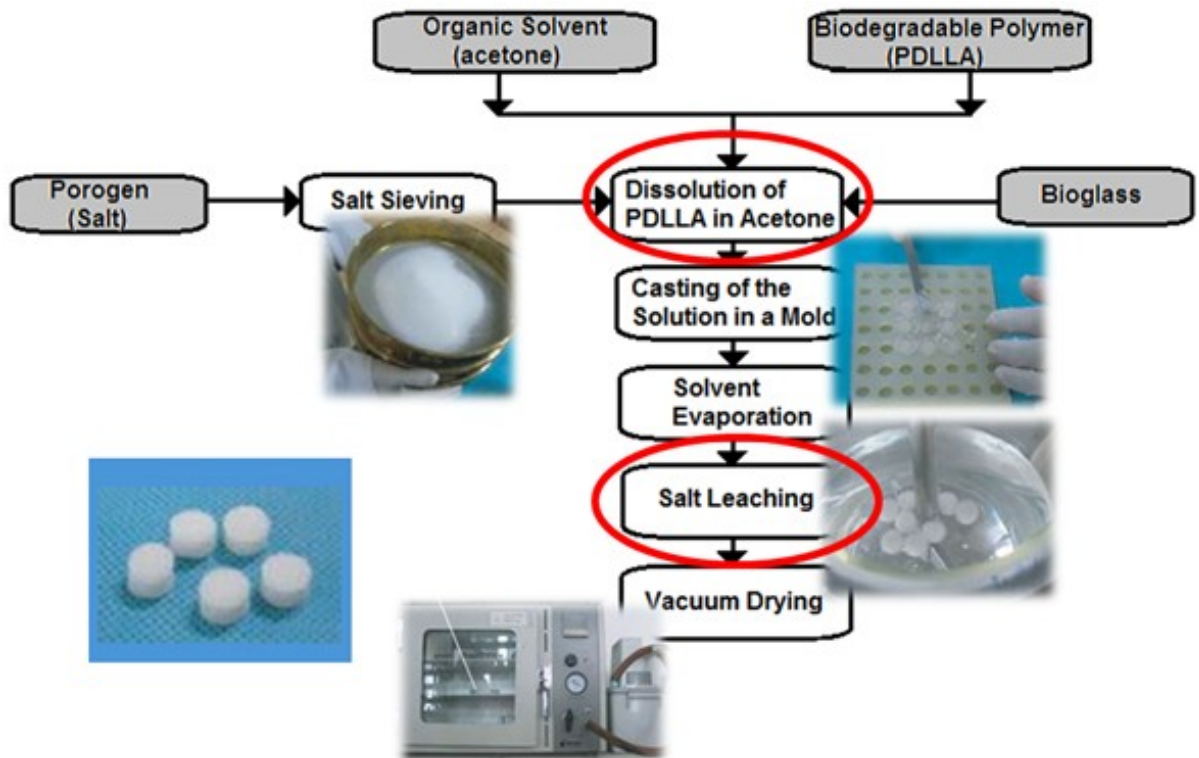


Fig. 3.3 – Scaffold Preparation by Solvent Casting/Particulate Leaching

Firstly, the polymer, PDLA, is dissolved in an organic solvent. The organic solvent chosen for this purpose is acetone because of its lower toxicity compared to other organic solvents such as chloroform. A 5% weight/volume ratio polymeric solution is created by mixing PDLA with acetone on a magnetic stirrer for two days. Subsequently, bioactive glass is added to the slurry. The amount of BG is 50:50 in relation to the weight of the PDLA. The porogen, salt, which was previously sieved to the desired scaffold pore size range of 75-355 μm , is next added to the mixture. The amount of salt is 94% in relation to the total weight of solid compounds. The homogeneously mixed paste is then cast in a mold where it solidifies (Fig. 3.4).

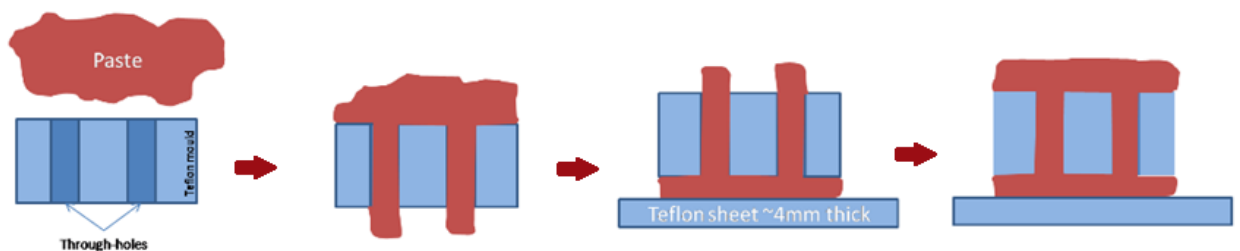


Fig. 3.4 – Scaffold Molding Step [Image provided with reprint permission by Martin A. Koch, PhD, Biomechanics and Mechanobiology group of the Institute for Bioengineering of Catalonia (IBEC)]

The mold is left under the fumehood and the solvent is allowed to evaporate for two days. Once removed from the mold, the scaffolds are immersed in distilled water to leach out the salt particles, creating hollow pores, for two days. During this period, the water in which the scaffolds are immersed is changed every six hours. To make sure there is no salt residue leftover, silver nitrate is added to an aliquot from the aqueous solution. If a white precipitate forms, there are still traces of salt and the leaching step must continue, but if no precipitate forms, all the salt has leached out and the scaffolds are ready to be

dried. The scaffolds are dried in a vacuum at room temperature for two days and finally stored in a desiccator until characterization.

3.2.4 Bioglass 45S5 Scaffold Extraction

BG was extracted out of the scaffold matrix by dissolving the polymeric structures in acetone. Specifically, scaffolds were immersed in acetone and the dissolution was helped by mixing with a magnetic stirrer for one day. After this, the acetone was decanted, the settled BG particles washed with the solvent, and lastly air dried.

3.2 Mold Preparation

Teflon

Teflon molds were made by drilling cylindrical holes in the desired scaffold dimensions (6.4 mm diameter x 12.86 mm height) in Teflon blocks. Figure 3.5 demonstrates one such block (Fig. 3.5a) and a PDLLA film (Fig. 3.5b) created to test the inertness of the Teflon molding material.

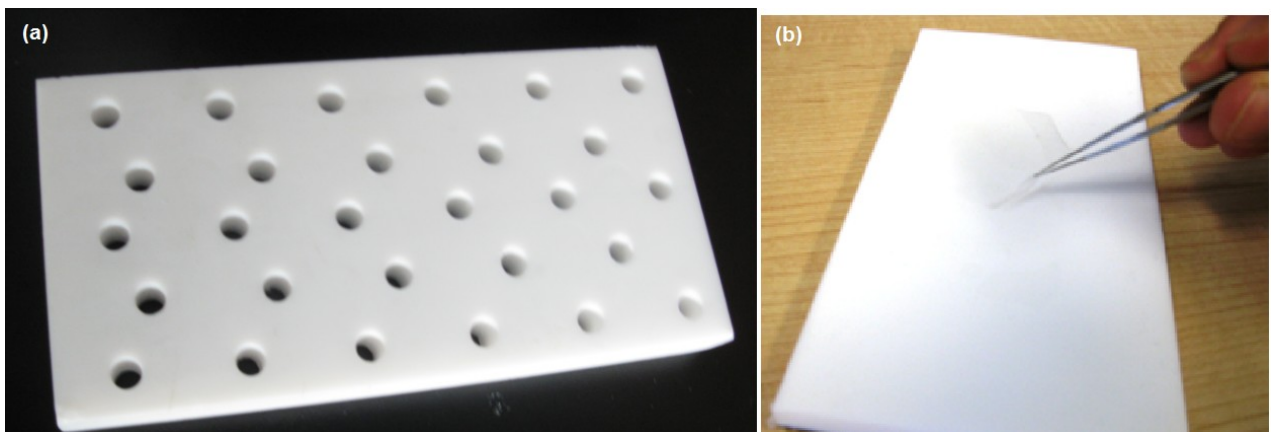


Fig. 3.5 – Teflon mold (a) PDLLA Film on Teflon (b)

Sil940

As Received

The Sil940 mold was fabricated as instructed by the manufacturer (Smooth-On, Inc.) by mixing the A, and B agents. The products were mixed in a 100A:10B weight ratio, vacuum degassed to eliminate any entrapped air, and finally poured in the molding container to cure at room temperature for 24 hours. Post curing, involved exposing mold to oven heat at 100 °C for 4 hours. After post-curing, the mold was taken out of the oven and air cooled. The mold cavities were finally thoroughly washed with dishwashing detergent to remove any product residues (Smooth-On, 2011b).

Lacquer Coating

The lacquer chosen for coating the Sil940 mold is depicted below (Fig. 3.6). This product is originally intended for application on furniture to add lustre. The lacquer is simply sprayed on one of the mold spaces on Sil940 (Fig. 3.6) and allowed to dry for 3 hours.



Fig. 3.6 – Coating Sil940 Substrate with Lacquer

Teflon Spray Coating

Sil940 was spray coated with Teflon spray (MS-122AD) similarly to the lacquer. This coating is originally intended to be used as release agent for application to mold plastics, rubbers, resins, acrylics, epoxies, urethanes, nylons, phenolics, polycarbonates, polystyrene, and elastomers (Miller-Stephenson Chemical Company, 2011).



Fig. 3.7 – Teflon Spray Coating for Sil940 Substrate

Teflon Tape Coating

Teflon tape was used to cover the surface of Sil940 such that the flexible mold backing is present, yet the polymeric paste does not come in contact with the silicone-based materials. Both a PDLLA film and a PDLLA/NaCl film were cast onto the sample test surface.

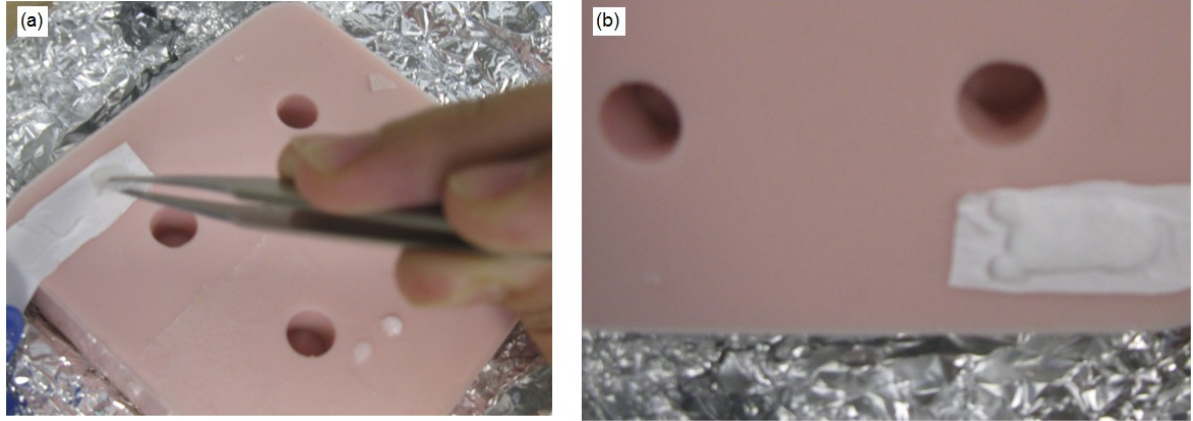


Fig. 3.8 – Sil940 Covered with PTFE Tape: PDLLA (a), and PDLLA/NaCl (b) films

Polyurethane

A sample polyurethane, urethane rubber ReoFlex series (Smooth-On, 2011b), molding substrate was provided, and a PDLLA solution was poured on the sidelines to create a film for XPS analysis (Fig. 3.9). The center of the sample in Figure 3.9 is used to create a PDLLA/salt film, which due to poor detachment was not further analyzed with XPS.

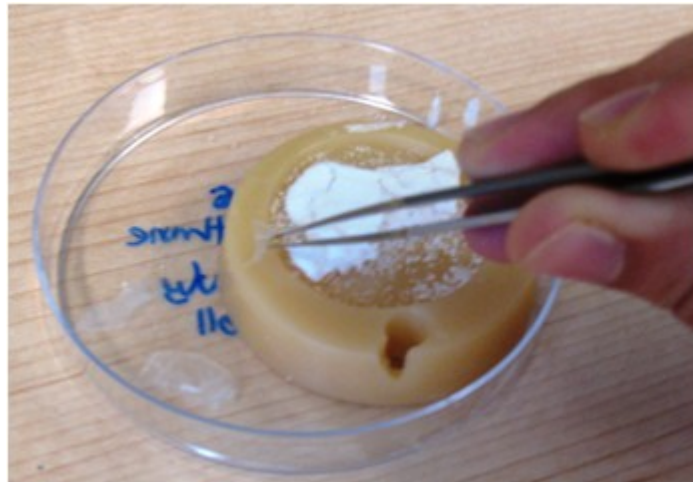


Fig. 3.9 – PDLLA Film Preparation on Polyurethane Substrate

Polyether

As Received

Polyether mold substrate, whose composition is given in Figure 3.10a, was fabricated using an automatic mixing unit (Pentamix™ 3 Mixing Unit). The mixture sets within minutes, and PDLLA solution was poured on the fully solidified polyether substrate to create a film (Fig. 3.10b).

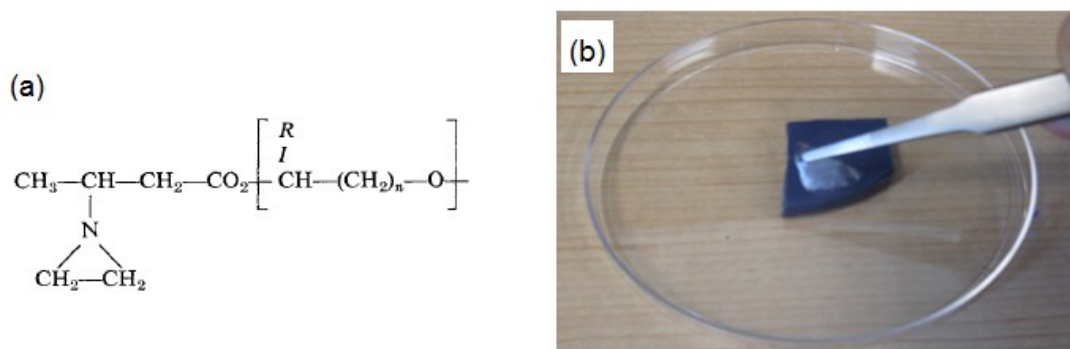


Fig. 3.10 – Polyether Substrate: chemical formula (a), and PDLLA Film Preparation (b)

Acetone Treatment

In an attempt to remove the silicone in the polyether cross-linking agents, the material was sonicated overnight in acetone, and subsequently washed. Once dried, a PDLLA solution was cast on its surface to create a film for XPS analysis.

Plasma Coating

Samples of polyether mold substrate were plasma coated. Three different types of plasma coating were tested for assessing their efficacy to prevent silicon leachate from the

polyether substrate (i) 30 minute hydrophobic and 15 minute hydrophilic, (ii) 30 minute hydrophobic, and (iii) 45 minute hydrophilic.

Polydimethylsiloxane (PDMS)

As Received

The PDMS substrate came as is and the substrate was not fabricated from raw materials. Both scaffolds and a PDLLA film were created from this substrate.

Ethanol Treatment, Acetone Treatment

In an attempt to possibly extract the silicon from the PDMS material, one mold was sonicated overnight in acetone and another in ethanol. Subsequently PDLLA solution was cast on each to create films that can be characterized by XPS spectroscopy.

4 – Results & Discussion

This chapter presents and discusses the results of the steps outlined in the previous chapter to (i) determine the transformation of Bioglass 45S5 during scaffold processing, and (ii) select the most suitable mold material for scaffold design.

4.1 Bioglass Transformation

4.1.1 Bioglass 45S5 Preliminary Characterization

Bioglass 45S5 Particle Size Analysis

As determined from the particle sizing analysis (Table 4.1), the average particle size for BGA and BGB are $75 \pm 49 \mu\text{m}$ and $150 \pm 43 \mu\text{m}$, respectively. Acetone and water, which are the fluids that come in contact with BG during the scaffold processing steps, do not affect the particle size (Fig. 4.1). Hence, we conclude that the BG particle size is unlikely to be altered during scaffold processing.

Table 4.1 – As received BG Particle Size

BGA	$75 \pm 49 \mu\text{m}$
BGB	$150 \pm 43 \mu\text{m}$

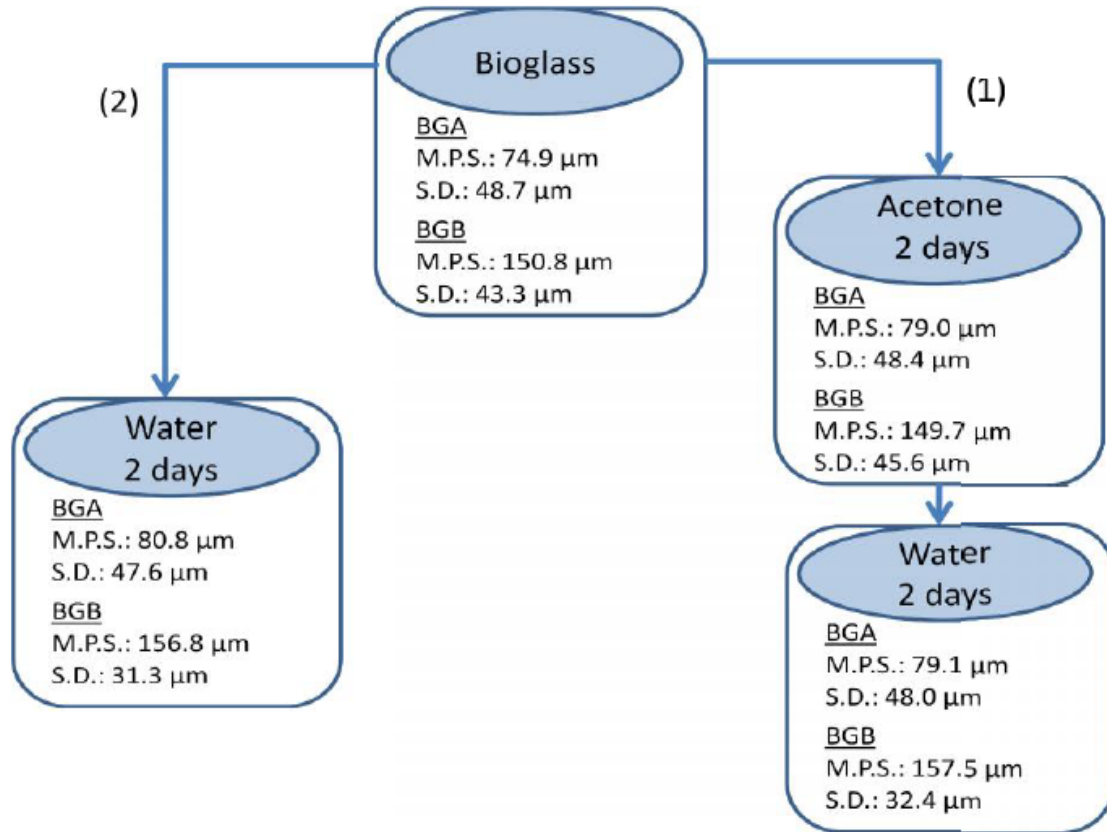


Fig. 4.1 – Bioglass 45S5 Particle Size Analysis: Mean Particle Size (M.P.S.) and Standard Deviations of as received, 2 days water, 2 days acetone, and 2 days both water and acetone treatments (S.D.)

Fourier Transform Infrared Characterization of Bioglass 45S5

A major part of the preliminary analysis involves analyzing whether and how Bioglass, the powder itself, reacts after acetone treatment, and also after an acetone treatment followed by a water treatment. Therefore, to begin with, the behaviour of BG particles in the fluids with which it comes into contact with throughout the scaffold processing will be monitored. For this purpose, characterization is done via FTIR a technique that analyzes the top 1-5 μm thick sample layer. Figure 4.2 shows three spectra; the first is the BGA as received (black), followed by the BGA treated two days in acetone (red), and finally the BGA treated two days in acetone followed by two days in water (blue). When

looking at the spectra of the BG that is additionally treated in water, there is some change such as the shift in the maximum position of OH band around 3400 cm^{-1} . A significant change is also visible in the 1570 cm^{-1} region. From literature (Cerruti, Greenspan, et al., 2005), this region is associated with the C=O vibration, which is attributed to the carbonates formed on the surface of the glass. However, it seems that the single peak in this region for the as received BG becomes a double, shorter, peak in the treated (acetone, water) BG. In fact, Cerruti et al. (2005) show that a single peak in the 1570 cm^{-1} region is associated with a silica-sodium environment whereas a double peak is an indication of a silica-calcium one (Fig. 4.3). This correlates with the BG dissolution mechanism (Fig. 4.6), once the BG is immersed in water, the Na ions leach out into solution and the Ca ions from the bulk of the BG migrate to the surface, hence resulting in the shift of the sodium carbonate (NaCO_3) peak to that of calcium carbonate (CaCO_3). The spectra of the acetone treated BG have only minor differences compared to the ones for the water spectrum. Taken together, these results indicate that BG does not react in acetone.

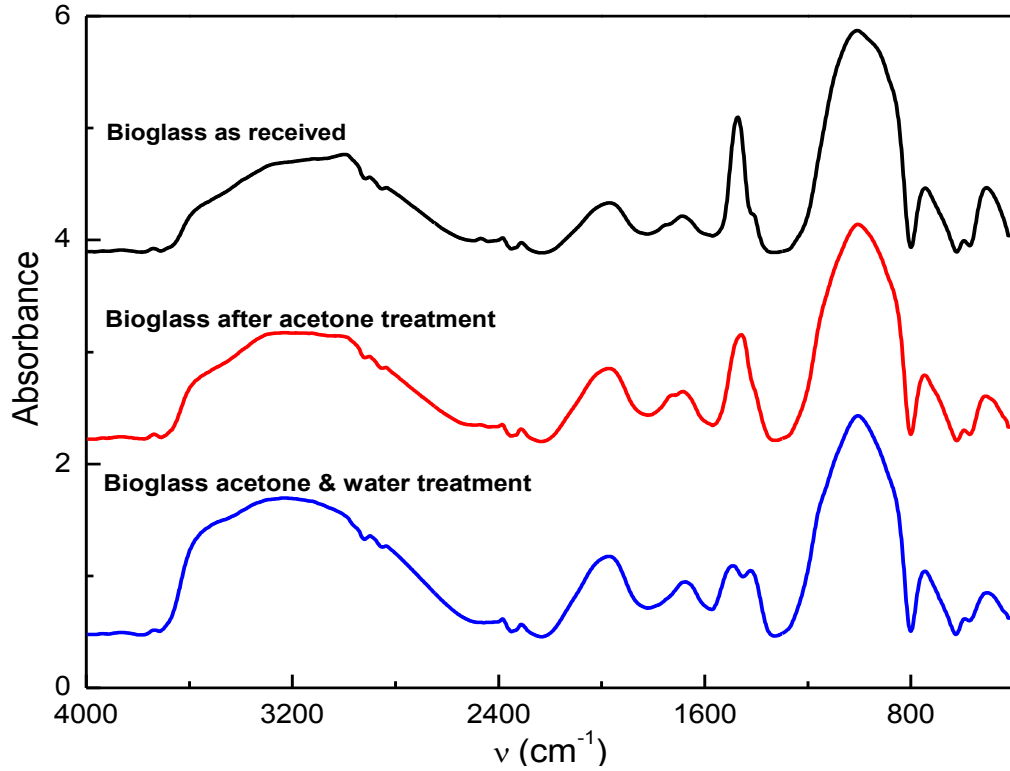


Fig. 4.2 – FTIR transmission spectra of BGA: as received (black), after acetone treatment (red), and after both acetone and water treatments (blue)

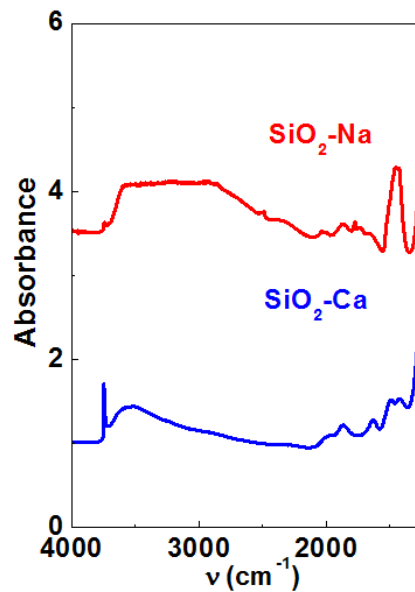


Fig. 4.3 – FTIR transmission spectra of silica doped with: sodium (red), and calcium (blue) (Cerruti, Greenspan, et al., 2005)

Elemental Release during Bioglass 45S5 dissolution, an ICP-OES analysis

Elemental release behaviour of BG in deionized water was determined with ICP-OES analysis (Table 4.2-4.5). The as received BG particle dissolution measurements were done after a similar time period as the BG inside the scaffolds during fabrication. Specifically, the elemental release for the as received BG was recorded after two days immersion in water, and after two days in water preceded by two days in acetone. Results conform to the mechanism of BG dissolution reported in literature (Cerruti, Greenspan, et al., 2005; Hench, et al., 1973). There are clear differences in BG elemental release as outlined below:

- a) The release for BGA is higher than BGB in water, which for Na correlates with the faster release of ions from smaller particles. It is interesting to note that such a difference is not visible for Ca possibly because there is already the formation of a Ca/P thin layer on the surface of these samples (which was not detected via FTIR). Thus, some Ca and P may have been released but already re-precipitated.
- b) The concentration of P is barely detectable, which can be attributed to the immediate supersaturation of the solution with calcium phosphate compounds, and precipitation of a layer of calcium phosphate before two days.
- c) Although acetone does not generate major changes in the FTIR spectra, the release behaviour seems to indicate some differences for BGB sample. This is an interesting observation that deserves further analysis.

Table 4.2 – BGA “2 days water immersion” water

Element	Na	Ca	Si	P
Average concentration [ppm]	51.1	17.5	45.1	0
Standard deviation [ppm]	1.40	0.08	0.60	0.02

Table 4.3 – BGB “2 days water immersion” water

Element	Na	Ca	Si	P
Average concentration [ppm]	27.6	17.1	38.0	0
Standard deviation [ppm]	0.30	0.40	0.90	0.03

Table 4.4 – BGA “2 days acetone, 2 days water immersion” water

Element	Na	Ca	Si	P
Average concentration [ppm]	59.4	19.8	53.6	0
Standard deviation [ppm]	0.60	0.40	0.80	0.07

Table 4.5 – BGB “2 days acetone, 2 days water immersion” water

Element	Na	Ca	Si	P
Average concentration [ppm]	58.4	30.9	74.6	0.04
Standard deviation [ppm]	1.50	0.10	1.20	0.01

pH Monitoring of Bioglass 45S5 dissolution

pH measurements at regular intervals during the first five and a half hours (330 minutes) of BG dissolution have been monitored (Fig.4.4). Results show a sudden rise in pH within the first minutes of dissolution, which gradually reaches a plateau. The trend is similar for both BG sizes.

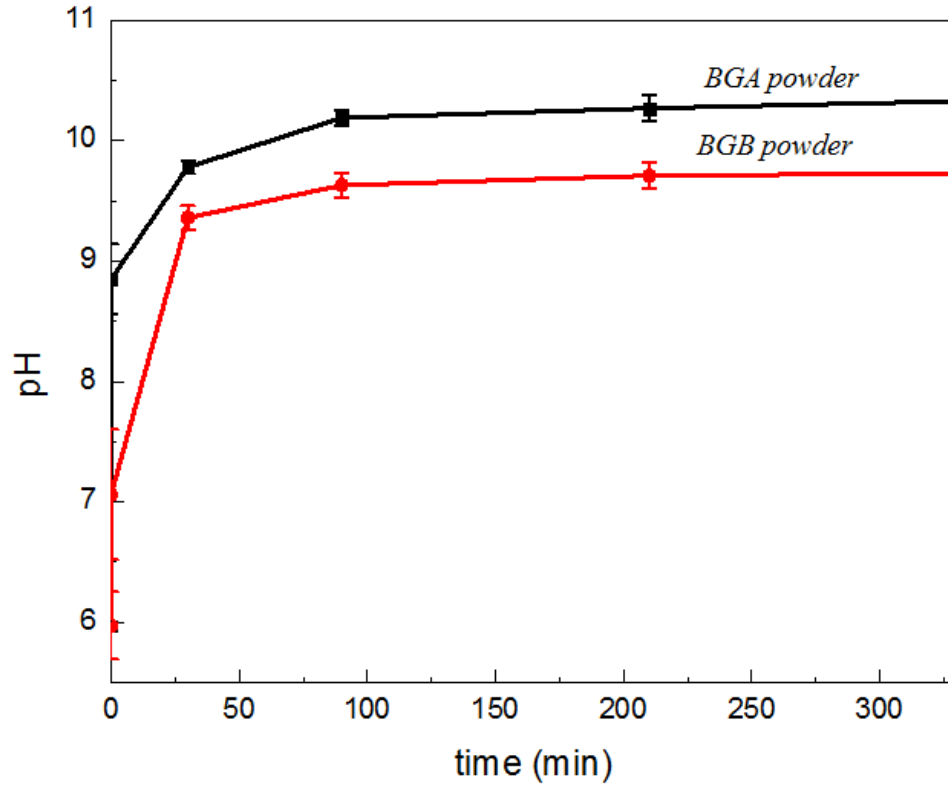


Fig. 4.4 – pH effects of Bioglass 45S5 dissolution

Similar to the elemental release profile, the pH increase complies with the mechanism of BG dissolution reported in literature (Hench, et al., 1973; Cerruti, et al., 2005). As previously mentioned, during the first stage of BG reactivity (Fig. 4.10), sodium ions leach out of the glass in exchange for hydrogen ions in solution that binds to the non-bridging oxygens on the BG surface (Fig. 4.5). The decrease in the concentration of hydrogen ions in solution, therefore, contributes to an increase in the pH of the solution.

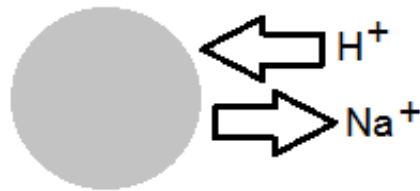


Fig. 4.5 – Bioglass 45S5 ion exchange in solution

4.1.2 Scaffold Characterization & the Effect of Bioglass 45S5 Addition

Scaffold Morphology

Scaffold with the intended dimensions of 6.4 mm diameter, and 12.86 mm height were created, and their morphology was assessed with SEM (Fig. 4.6). BG appears integrated within the polymeric matrix, which is an open-cell matrix, both porous and interconnected.

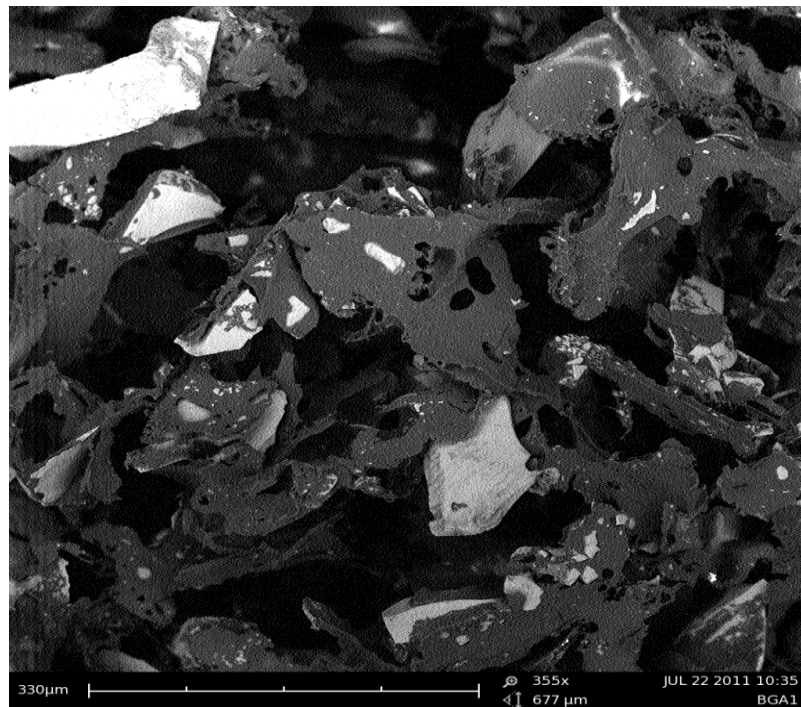


Fig. 4.6 – SEM image of PDLLA scaffold prepared using the solvent casting/particulate leaching technique with BGA

Scaffold Transformation Upon Bioglass 45S5 Addition

To analyze BG transformation within the scaffold, FTIR spectra of the PDLLA scaffolds both with and without BG were compared (Fig. 4.7). FTIR is primarily applied for a qualitative analysis and provides information on the complex bonding in matter (Biber &

Stumm, 1994; Payá, Monzó, Borrachero, Velázquez, & Bonilla, 2003; Robinson, 1995). Furthermore, the spectrum provides the means to determine if a given functional group such as a carbonyl group, in a molecule is present (Robinson, 1995). Although there are subtle differences between the two spectra, the main change of importance relative to the comparison in this study is a peak at $\sim 1630\text{ cm}^{-1}$. The latter can be attributed to the H-O-H bending vibration of water molecules (Cerruti et al., 2005). Thus, it is safe to deduct that the addition of BG resulted in a composite scaffold that is hydrated. However, major changes that could have occurred on the BG during scaffold processing are not visible on this spectrum probably because the intense peaks from PDLA overshadow those relative to BG.

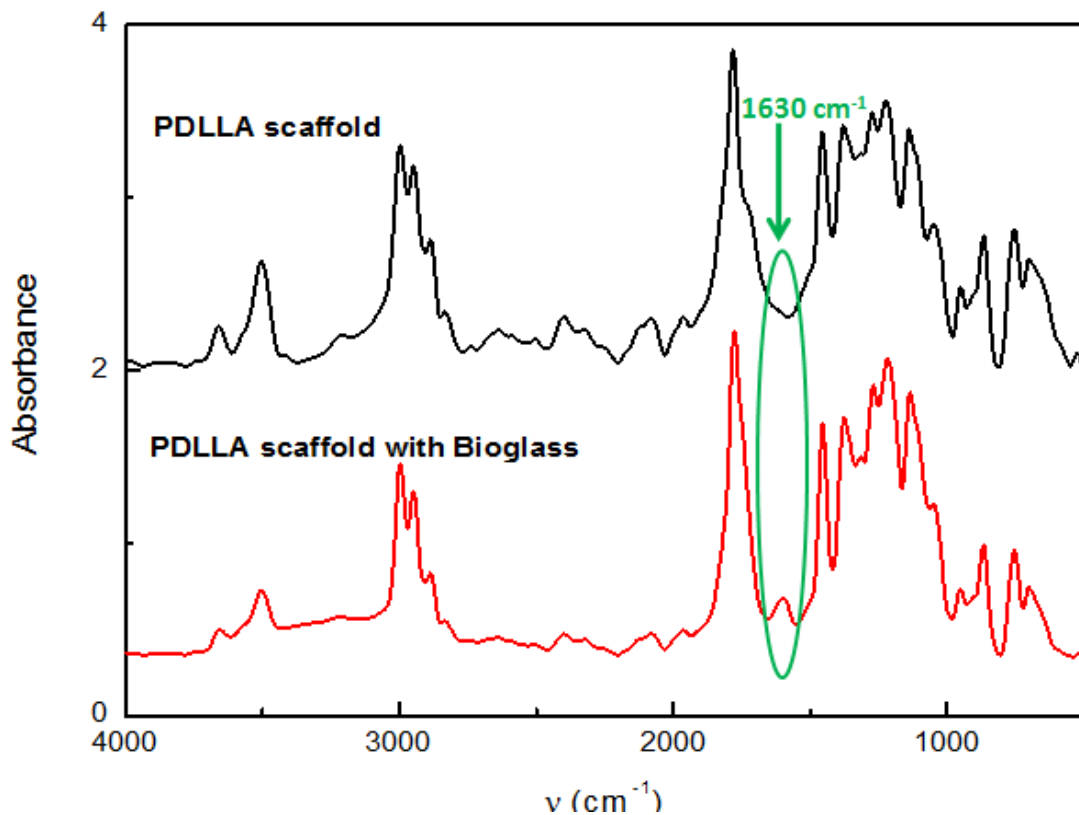


Fig. 4.7 – FTIR spectra of scaffold: PDLA matrix only (black), and Composite PDLA/BGA scaffolds

4.1.3 Bioglass 45S5 Transformation in Scaffold Processing

FTIR Analysis

Devising a technique to look at the BG inside the scaffold after processing was essential. During the preliminary BG analysis, it was found that acetone does not induce any significant changes to BG. Hence, the solvent can be used to extract out the BG from the polymeric scaffold matrix without affecting its properties. The following figure, therefore, demonstrates the FTIR spectra of not only the BGA as received, and treated, but as well that of the BG extracted (Fig. 4.8, Table 4.6). Several interesting observations can be made from these spectra obtained using the qualitative FTIR technique. Firstly, the same change in carbonate peak in the 1570 cm^{-1} region (Cerruti, Greenspan, et al., 2005) occurs as with the raw BG previously discussed (Fig. 4.2). Specifically, for both the treated BG and extracted there is a shift from the sodium carbonate single peak to the calcium carbonate double peak, which conforms with the first stage of BG reactivity (Fig. 4.10).

Table 4.6 – BG Designations

BG as received	Raw BG as obtained from directly from provider
BG treated	BG treated 2 days in acetone & 2 days in water (solutions involved in scaffold processing steps)
BG extracted	BG extracted from the scaffold

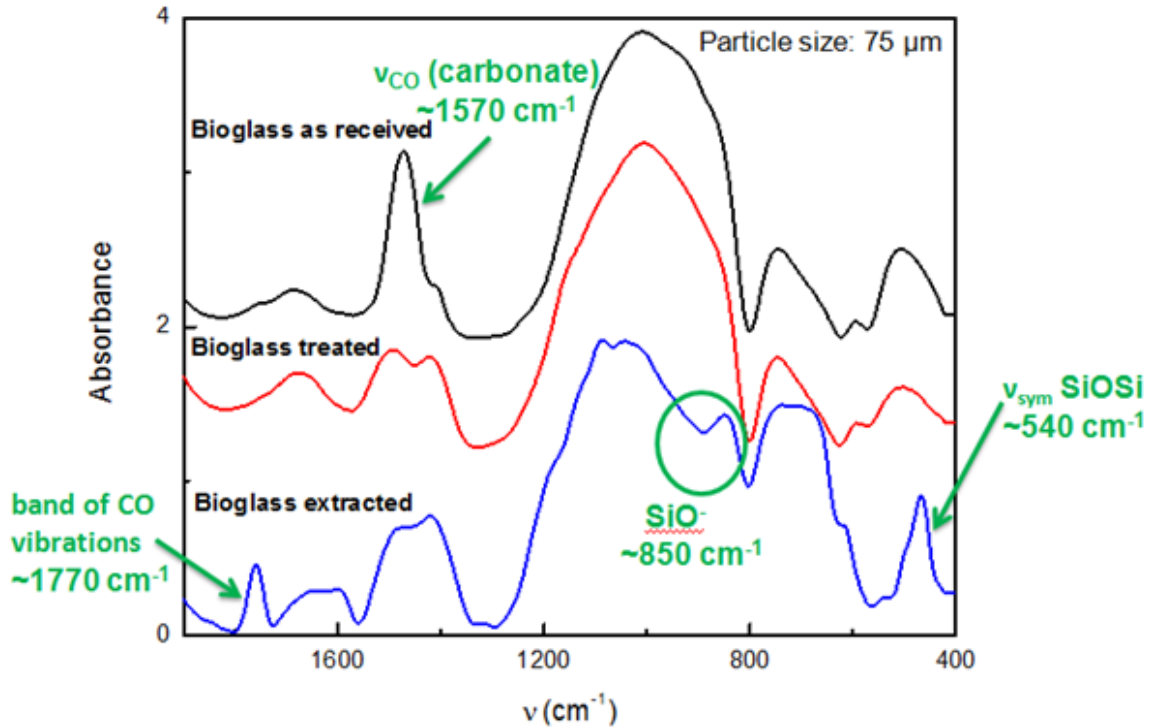


Fig. 4.8 – FTIR spectra of BGA: as received (black), 2 days acetone treated (red), and extracted from the scaffold (blue)

Interestingly, however, it appears that the BG extracted from the scaffold has reacted differently than the raw, treated BG. In particular, there is an extra peak at the $\sim 850\text{ cm}^{-1}$ region, which from literature (Cerruti, Greenspan, et al., 2005) is associated with SiO^- ; in other words silicon bound to non-bridging oxygens from SiOH formed during the first stage of reactivity of BG (Fig. 4.9a). Furthermore, the extracted BG from the scaffold has a peak at $\sim 540\text{ cm}^{-1}$, which results when there is symmetric Si-O-Si vibration (Fig. 4.9b), and is believed to be the result of the formation of a silica-rich layer as depicted in the second stage of reactivity of BG (Fig. 4.10).

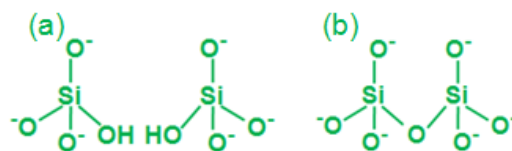


Fig. 4.9 – Chemical environment of Si in Bioglass 45S5 at different stages of reactivity

The differences and the appearance of an additional peak at $\sim 1770\text{ cm}^{-1}$, which can be attributed to the overtone band of CO vibrations (Nakamoto, 1986), indicate that overall the BG extracted from the scaffold has reacted further than the raw BG immersed in acetone and water. This observation, however, is counterintuitive because the BG inside the protective polymeric environment of the scaffold should react to a lower extent than the raw BG powder.

Stages of Reactivity when in body fluid...

- 1 Na⁺ ions leach out → SiOH formation
- 2 Formation of a silica-rich layer
- 3 Formation of a Ca-P rich layer
- 4 Crystallization of hydroxycarbonate apatite

Fig. 4.10 – Stages of Bioglass 45S5 reactivity (Boccaccini & Maquet, 2003)

FTIR spectra relative to BGB transformations are shown in Fig. 4.11. Although the extracted BG seems to have reacted to some degree as seen from the change in the carbonate peak in the 1570 cm^{-1} region (Cerruti, Greenspan, et al., 2005), this reactivity is not as extensive as for BGA. In fact, BGB extracted out of the scaffold seems to have reacted to a similar degree as when simply treated in acetone and water. In particular, there is no dramatic change in peak at $\sim 540\text{ cm}^{-1}$ (see inset of Fig. 4.11), which was indicative of a silica rich layer formation on BGA. In addition, there is a clear absence of the peak at $\sim 1770\text{ cm}^{-1}$, which was indicative of the CO stretches (Nakamoto, 1986). Hence, BGB extracted from the scaffold remains at an earlier stage of reactivity.

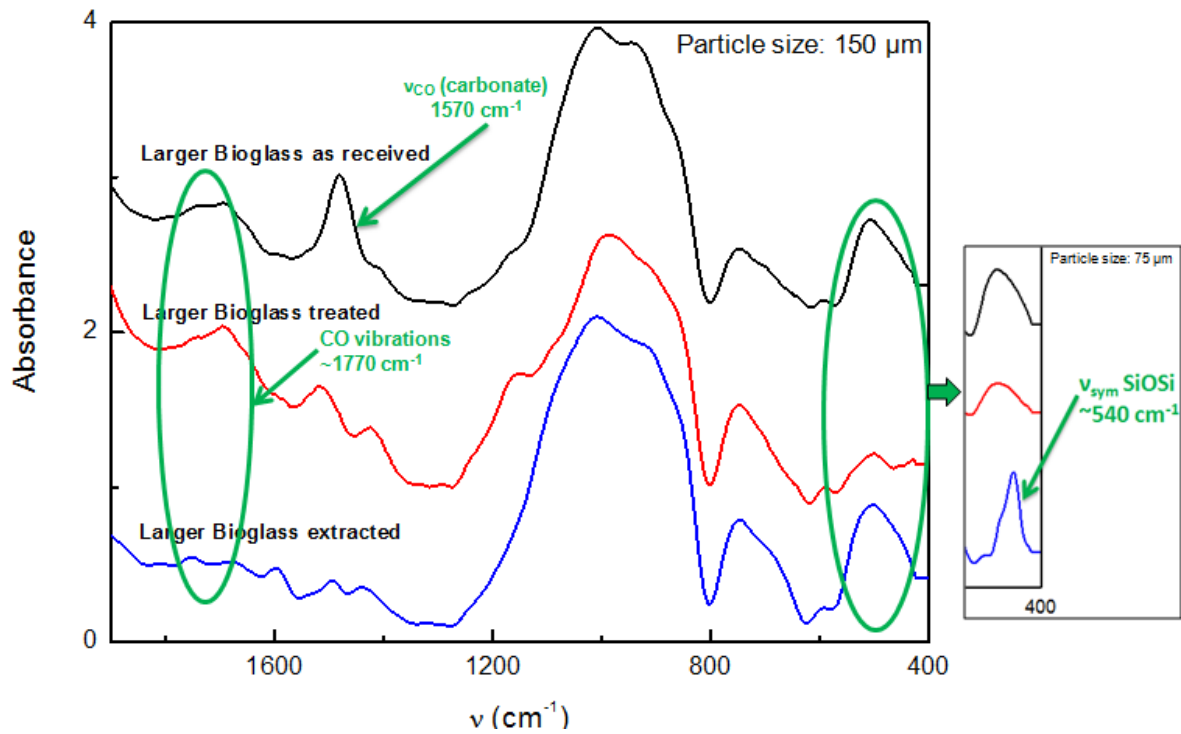


Fig. 4.11 – FTIR spectra of BGB: as received (black), 2 days acetone treated (red), and extracted from the scaffold (blue)

XPS Analysis

Then, the changes in chemical environment of selected elements were analyzed by collecting high resolution spectra. Figure 4.12 shows high resolution spectra for P_{2p} .

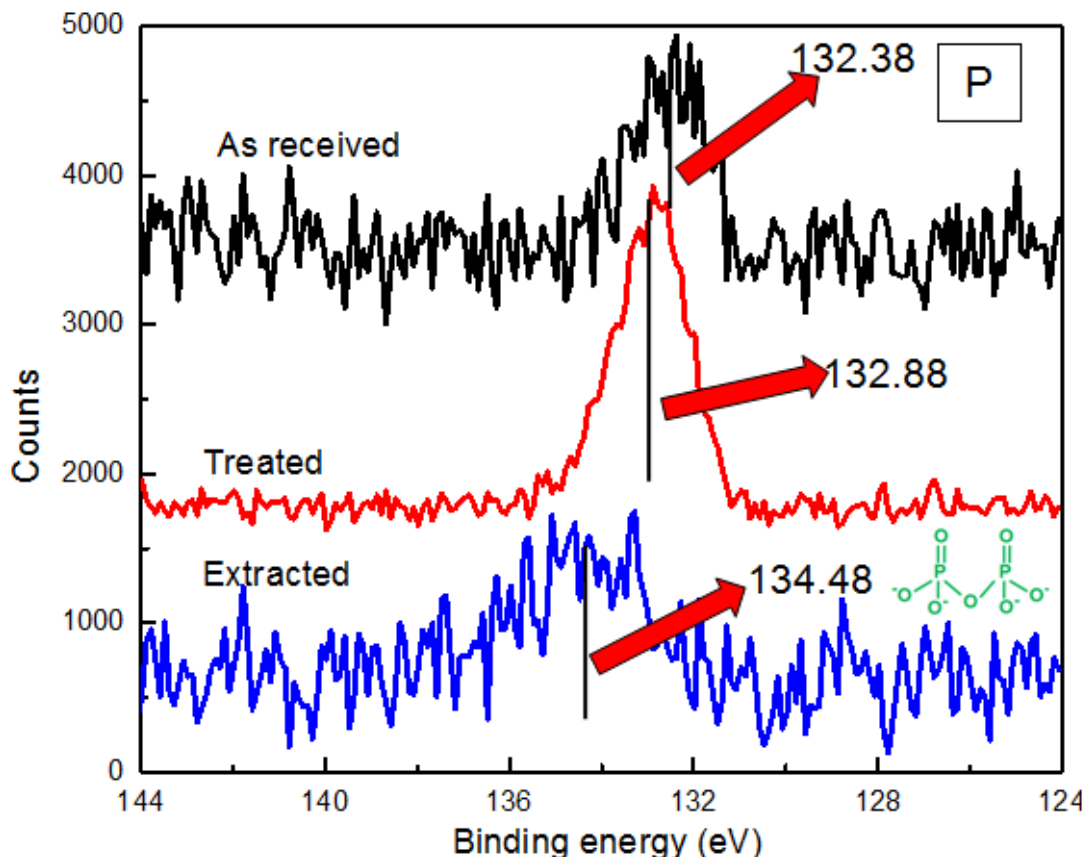


Fig. 4.12 – XPS spectra for phosphorus of BGA: as received (black), treated (red), and extracted (blue)

While the P_{2p} peaks on the as received BG and on the treated one both are at a binding energy of 132.6 eV, the P_{2p} peak on BGA extracted from the scaffold is at 134 eV. A peak at ~132 eV is indicative of phosphate ions in an isolated environment, whereas P_{2p} at ~134 eV is associated with a pyrophosphate ions (Briggs & Grant, 2003) (Fig. 4.13). This could be indicative of the fact that phosphate ions have accumulated on the surface of the extracted BGX, thus getting closer to each other and in a “pyrophosphate-like” environment. This is in agreement with the earlier FTIR spectra (Fig. 4.8), which showed that the BG extracted from the scaffold is at a more advanced stage of reactivity. XPS spectra would thus indicate that P ions have started migrating from the bulk to the surface of the glass.

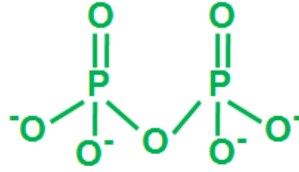


Fig. 4.13 – Phosphorus in pyrophosphate-like environment

In addition to P, we looked at the high resolution XPS of silicon (Fig. 4.14). While the Si_{2p} peaks of the as received and treated BGA are at around ~102 eV, which is associated with Si in silicate ions (Briggs & Grant, 2003) the peak for the treated sample is found at ~104 eV, which is ascribed to Si-O-Si, in other words Si in a Si rich layer (Briggs & Grant, 2003).

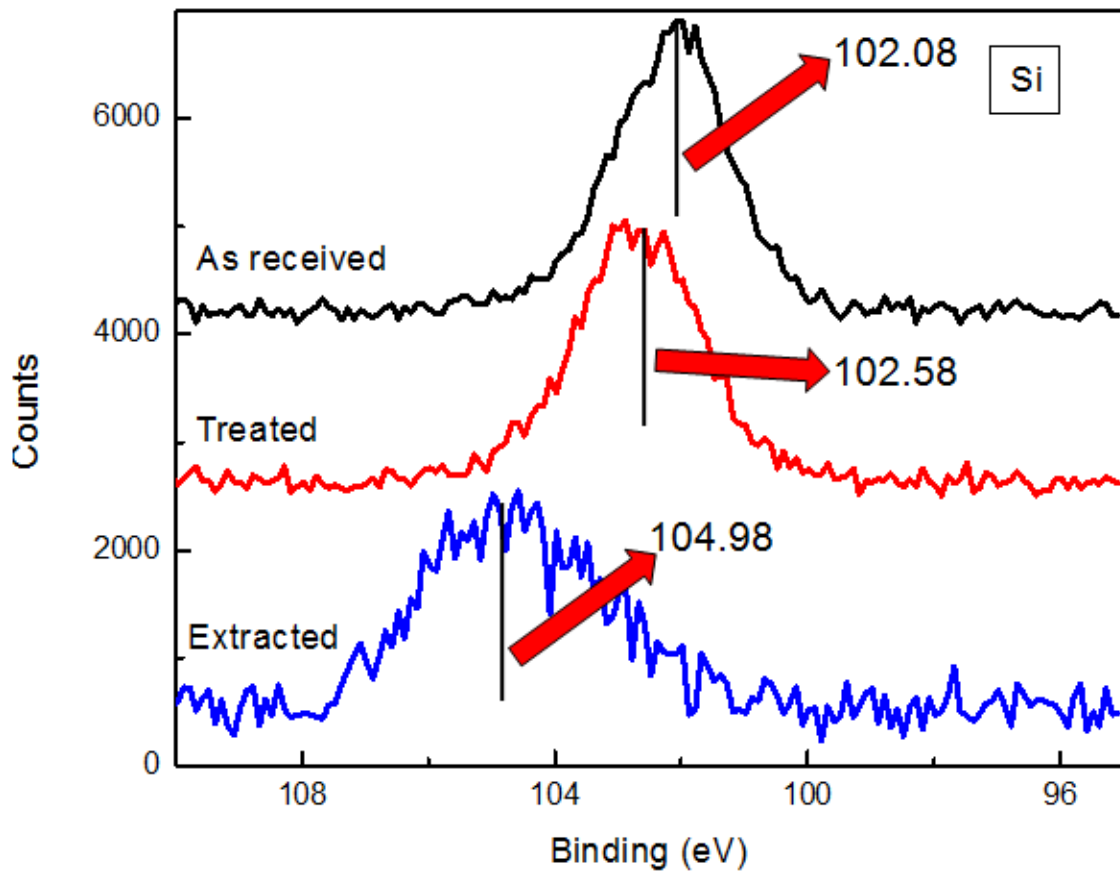


Fig. 4.14 – XPS spectra of silicon for BGA: as received (black), treated (red), and extracted (blue)

Hence, the Si_{2p} XPS spectra further confirm that the extracted BGA being at a more advanced stage of reactivity. Specifically, the Si detected on the surface of the as received and treated BG is bound to non-bridging oxygens, as in the step where SiOH groups are formed, whereas once the BG is processed in the scaffold, the Si on its surface is in a silica-rich layer environment, similar to the second step of BG reactivity (Fig. 4.10). In conclusion, both the FTIR and XPS data indicate that the extracted BG is at a more advanced stage of BG reactivity.

pH Effects

In an attempt to understand why BG reacts more when surrounded by PDLLA, we measured the pH of the solutions from dissolution experiments over an approximate five-hour period (Fig. 4.15). Firstly, the pH of raw BG of two different sizes was monitored. Similarly to the BG preliminary analysis (Fig. 4.4), the pH of the BG solution quickly rose and then stabilized. This is concurrent with the mechanism of BG reactivity (Fig. 4.10): the first step involves release of sodium ions from the glass followed by an uptake of hydrogen ions from the solution that results in SiOH formation on the surface of the glass. Therefore, if there is an uptake of hydrogen ions from the solution, then the pH of the solution will increase. The pH of the dissolution of PDLLA scaffold alone was also monitored—in other words, the polymeric scaffold without addition of BG. It appears that the pH is relatively stable at 5.5. This is the same value that we measured for DI water, indicating that no reaction occurs on PDLLA immersed in water for 5 hours. This is in agreement with PDLLA degradation, which occurs over weeks (Oh, Nam, Lee, & Park, 1999; Patterson, Stayton, & Xingde, 2009), and thus the lactic acid degradation product

cannot have been released to a significant amount in the short term period of only ~5 hours.

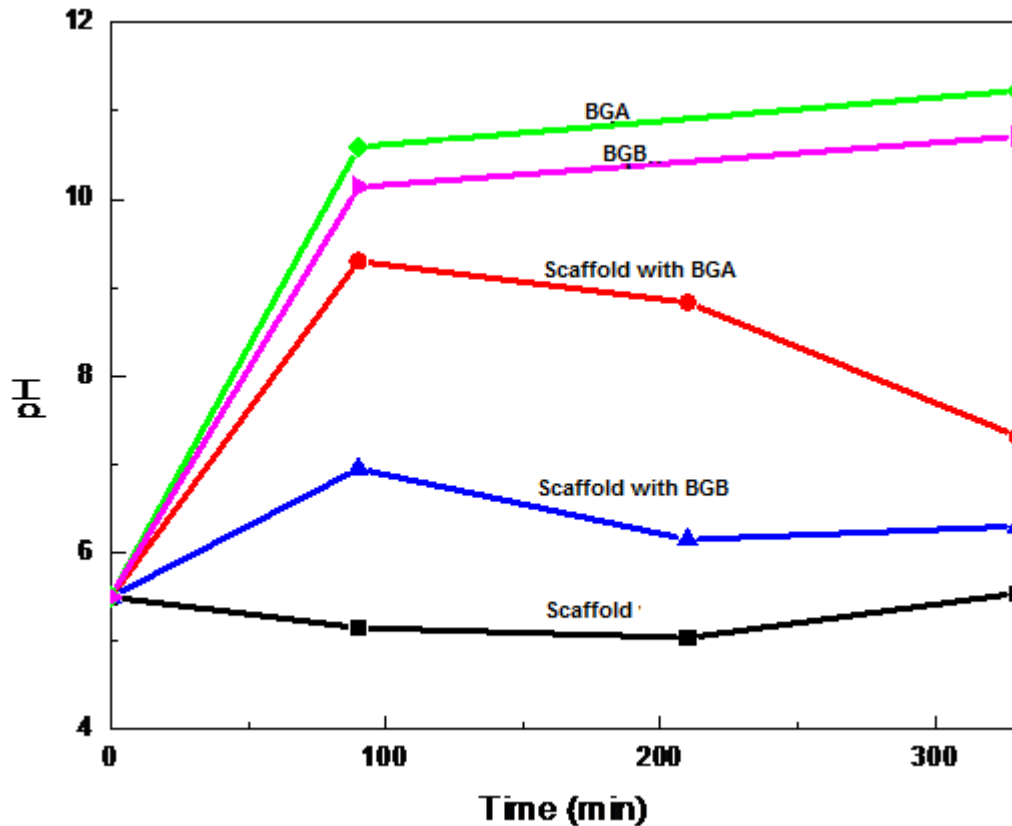


Fig. 4.15 – The pH effect: Bioglass 45S5 and scaffold dissolution experiments

The pH of composite PDLA-BG scaffold solution was also measured. After an initial increase, sharper for the scaffold containing the smaller size BG, the pH reached a value of 6.5 for PDLA-BGB and 7.5 for PDLA-BGA after 2 hours of dissolution. Studies on BG reactivity at different pH (Cerruti, Greenspan, et al., 2005) show that a layer of hydroxycarbonate apatite forms on BG surface when the solution pH is about 7.4. Therefore, extracted BG reacted further than the treated, probably because the polymeric environment slows the BG dissolution, which results in the transfer of less hydrogen ion from the solution to the BG surface. The result is a pH of the envrioning solution closer to

that favourable for BG reactivity, and hydroxycarbonate apatite formation, namely a 7.4 pH (Cerruti, Greenspan, et al., 2005). The polymer could have also been modified during processing and it can potentially be an important factor in the lower solution pH, but further investigation with this regard is required.

4.2 Mold Material for Scaffold Design

Teflon

As depicted in Figure 4.16, scaffolds cast into the Teflon mold largely retain their structure, yet possess uneven edges, and at times break during scaffold removal. Overall it is hard to obtain a full batch of consistent size. BG transformation within the polymeric matrix is dependent on the scaffold's contact area with the immersing solution during processing. Therefore, although the best is done to monitor this transformation and conduct the characterization with scaffolds of the same approximate size, a potential source of error is introduced because of non-uniformity in the scaffold shape.

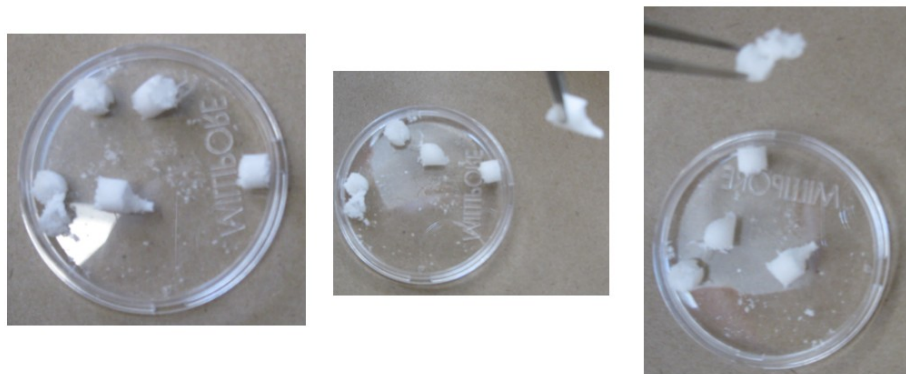


Fig.4.16 – Scaffolds Prepared in Teflon Mold

Sil940

The Sil940 molding material is quite flexible, and scaffolds smoothly pop out of the mold without much effort. Therefore, from a physical point of view, the mold made from this material is ideal. However, XPS characterization of the surface of the PDLLA film cast on Sil940 shows an average of 20.1 At.% of Silicon (Appendix B.1). The material reacts with acetone, and results in Si leachate on the polymeric film. Hence, Sil940 cannot be used as is for designing mold to cast the scaffold paste. However, due to its ease of fabrication, smooth structure and flexibility, it is further investigated with a lacquer coating, Teflon spray coating, and PTFE (Teflon) tape covering.

Sil940 with Lacquer Coating

Figure 4.17 depicts a scaffold prepared in the Sil940 mold spray coated with the lacquer. Although the scaffold is as easily extracted from the mold with the coating as it is without, the lacquer detached from the substrate surface and visibly stuck to the scaffold (see scaffold tip pointed by blue arrow).



Fig. 4.17 – Scaffold Prepared in Lacquer Coated Sil940 Mold

This result was predictable as the coating, once dried, could easily be peeled off, and in fact, tests showed that a small piece of it quickly dissolved in acetone within minutes (Fig. 4.18).



Fig. 4.18 – Deteriorated Lacquer Coating on Sil940 Mold

Sil940 with Teflon Spray Coating

Sil940 coated with Teflon spray is not much promising either. To begin with, similar to the lacquer coating, once dried, the sprayed on Teflon coating is easily smudged by touch. Secondly, XPS results demonstrate that in addition to silicon, fluorine is transferred to the PDLA sample film from the coating. The presence of these elements even prevails to depth of at least 15 nm, as demonstrated in high resolution XPS analysis (Ta205=0.25 nm/s; PDLA=1 nm/s, total of 3 levels) after etching the film surface (Fig. 4.19). Note that the high energies at which the Si and F peaks showing the spectra in Figure 4.19 are related to sample charging (no energy calibration was performed during this analysis).

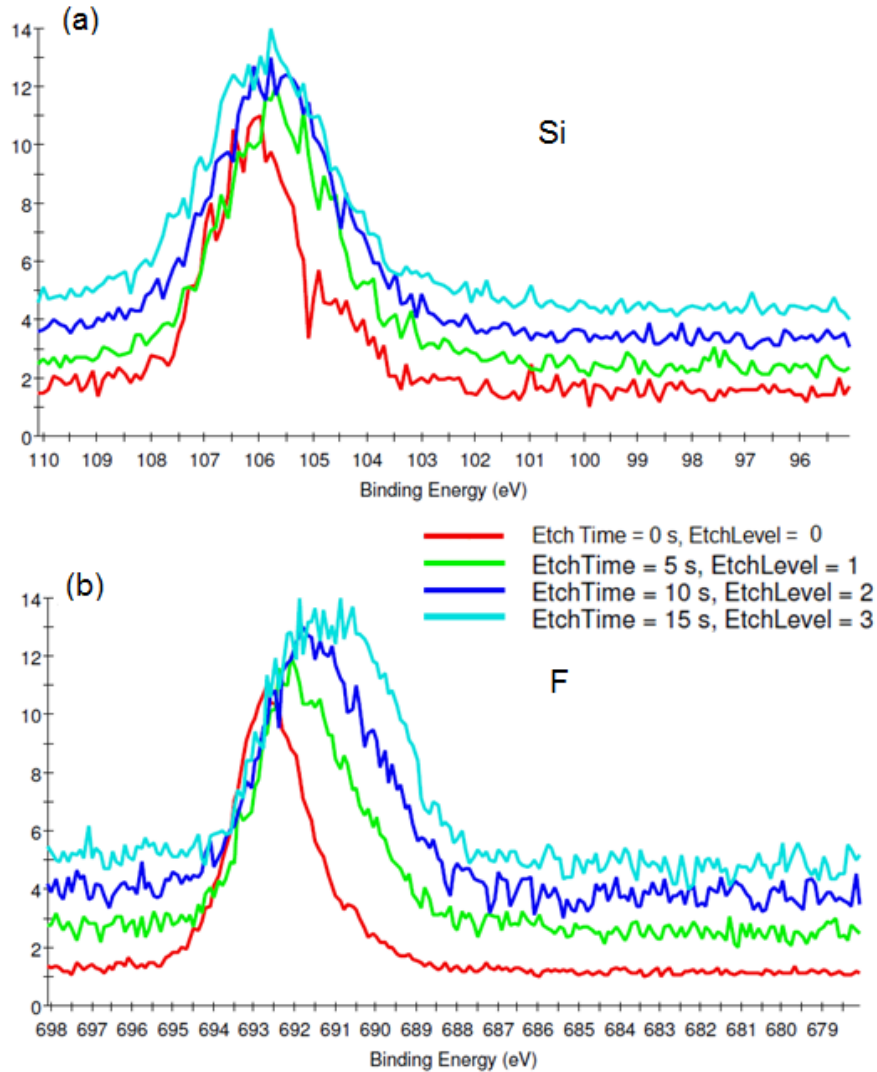


Fig.4.19 – High Resolution XPS Analysis of PDLLA Film Cast on Teflon Spray Coated Si1940

Sil940 with Teflon Tape Covering

Firstly, unlike for the Teflon mold, the scaffold made on the Si1940 with Teflon tape covering does not break and can be easily removed. However, depending on the thickness of the tape and the way the deep, hollow hole in the mold is covered, the resulting scaffold can have with non-uniform edges (Fig. 4.20). Another issue is covering the Si1940 with PTFE tape in the first place because the surface is slippery and the process is

not efficient with respect to the time spent and uniformity of the final product. Rather than a PDLLA film, a PDLLA/salt film was tested because the former practically became one with the tape and its edges were hard to distinguish and peel off. XPS characterization shows presence of 5.9 At.% silicon on the film, which although is less than that of the as is Sil940 substrate (20.1 At.%), still remains significant. Therefore, Sil940 with Teflon tape covering fails as a suitable molding medium if not for the difficulty to maintain the tape straight and properly cover the slippery mold, at least for the silicon detected on the sample surface.



Fig. 4.20 – Sil940 PTFE tape covered scaffold

Polyurethane

Although flexible, PDLLA films were hard to detach from polyurethane. Thus, despite the flexibility of polyurethane, a mold of this material will similarly to the Teflon be problematic during scaffold removal. In addition, SpillTech (2011) shows that polyurethane is incompatible with acetone (SpillTech, 2011).

Polyether

As shown in Figure 3.10a, silicon is not an element part of the inherent composition of polyether, but is within its crosslinking agent. Polyether is flexible and XPS results show that although silicon leaches out from the material onto the sample, the amount (2.2 At.%, see Appendix B.2) is much lower than other investigated materials such as Sil904 (20.1 At.%). Thus polyether can be potentially promising with further treatments or coating, which may remove the silicon-containing agents or create a barrier for silicon transmission. Acetone treatment of polyether was not successful at removing the silicon-containing cross-linking agent. However, plasma treated polyether can be used as molding material because XPS results do not show any trace of silicon leachate on the samples and hence this surface modification appears to work as preventative barrier.

Polyether after Acetone Treatment

Polyether slightly swelled after overnight sonication in acetone. The PDLLA film cast on this swelled substrate could not be removed, hindering subsequent XPS characterization. Therefore, acetone undermines the integrity of polyether.

Polyether after Plasma Coating

After 45 minutes of hydrophobic plasma treatment, the PDLLA film made on the polyether shows no sign of silicon. An example of the XPS elemental survey of one of the points on PDLLA film cast of the plasma coated polyether is shown in Fig. 4.21. The intense peaks of carbon and oxygen are clearly visible. However, there is a clear absence of silicon whose peak, if present, would be situated in the lower region at ~100 eV depending on its chemical environment (Briggs & Grant, 2003).

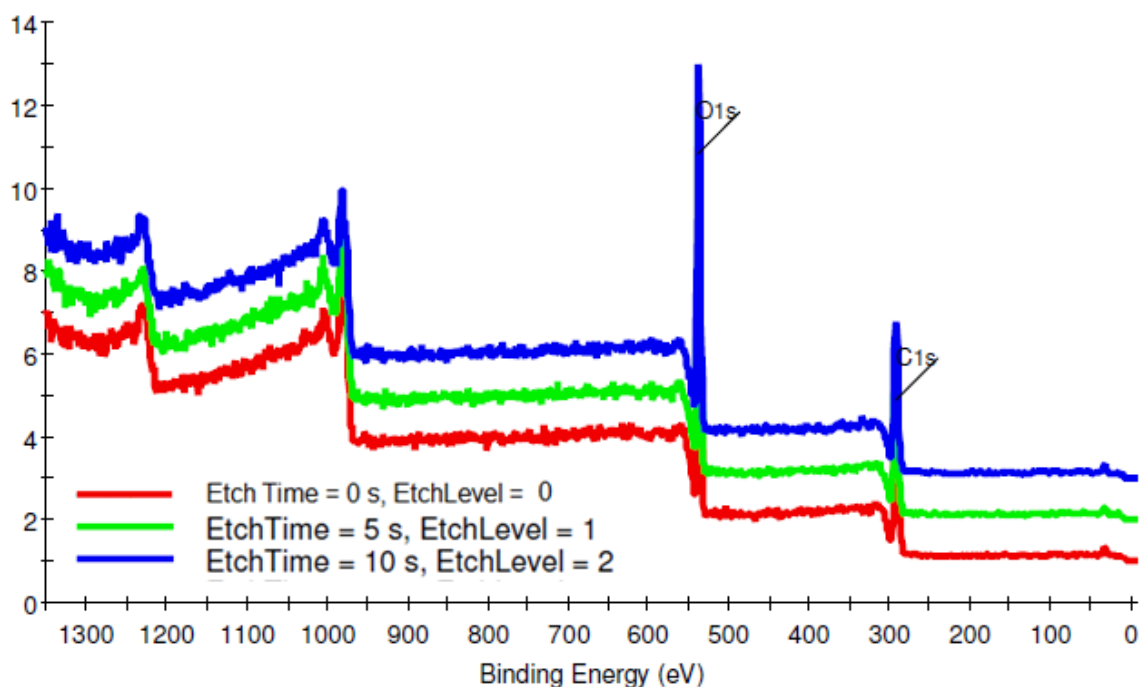


Fig. 4.21 – XPS Elemental Survey of PDLLA film cast on plasma Coated Polyether

Furthermore, high resolution XPS of silicon confirms the absence of this element even after etching the PDLLA film surface up to a depth of 15 nm (Fig. 4.22). Hence, plasma treatment of the polyether substrate is an effective means to prevent silicon penetration on samples; this surface modified material can be a potential candidate for designing scaffolding molds.

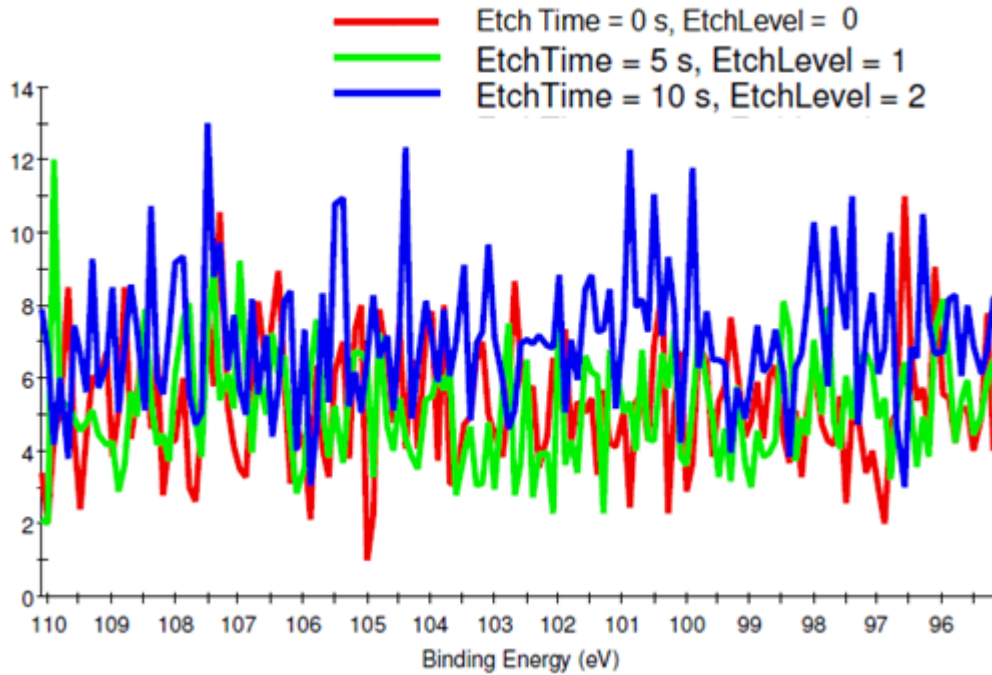


Fig. 4.22 – XPS Si High Resolution Spectra of PDLA film on plasma Coated Polyether

Polydimethylsiloxane (PDMS)

Uniform edge scaffolds made using a PDMS mold could be easily extracted (Fig. 4.23). Since the material is already being used in microfluidics components for biomedical applications, there is a chance that it is inert and will not result in silicon leachate. However, 13.9 At.% silicon is detected on PDLA films made on the PDMS substrate (Appendix B.3). Similar to polyether, the amount of silicon is much less than Sil940 and there could be a potential to remove the silicon through treatments such as in ethanol or acetone.

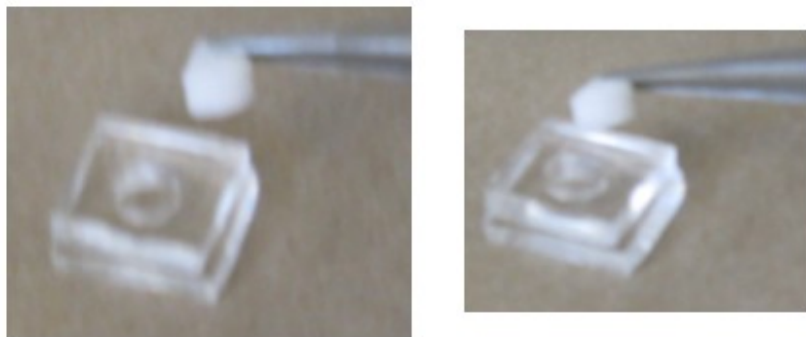


Fig. 4.23 – Scaffold Prepared in PDMS Mold

PDMS after Ethanol Treatment

Overnight ethanol treatment does not eliminate silicon from PDMS, and PDLLA films made on the surface of this substrate result in a 7.74 At.% silicon content. XPS depth profiling confirms that silicon remains on the sample after three layers of etching, totalling about 15 nm in depth (Fig. 4.24). The energies on these spectra are miscalibrated because of surface charging.

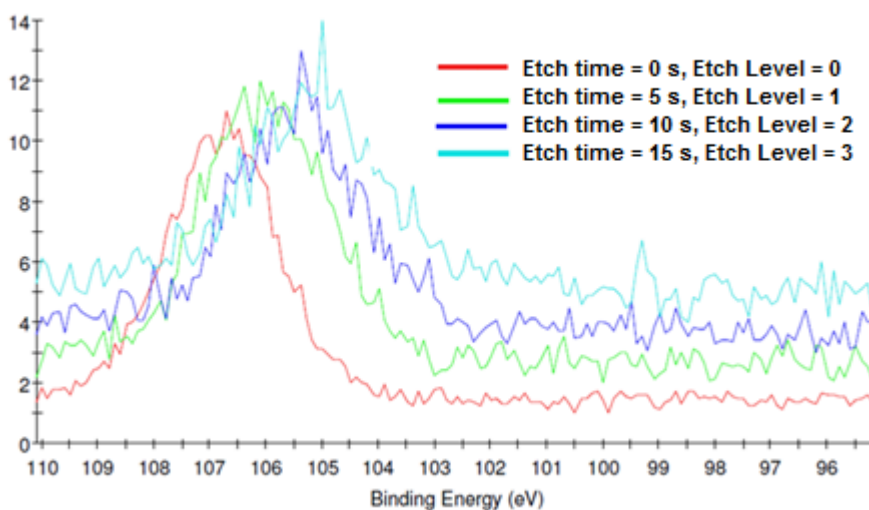


Fig. 4.24 – XPS High Resolution Si Spectra with Etching (~1 nm/s) on PDLLS film prepared on ethanol treated PDMS substrate

PDMS after Acetone Treatment

PDMS sonicated overnight in acetone results in a lower amount of silicon, 3.6 At.%, on the PDLLA film (Appendix B.4). This is an improvement in comparison to the as received and ethanol treated PDMS. Nevertheless, presence of this element is detrimental for cells. Additionally, silicon is one of four main compositional elements (Ca, Na, P, Si) of BG that is involved in the stages of BG dissolution and hydroxyapatite formation. As a result, any amount of silicon transferred from the mold to the polymeric film surface can interfere with the characterization of BG reactivity within the scaffold. Therefore, regardless of the treatments and despite its common use for microfluidics components, PDMS is not a suitable molding material.

5 – Conclusion & Summary

The purpose of this final chapter is to tie all aspects of the study together by providing a summary of the goals and achievements, as well as provide a conclusion based on the results obtained in the investigation. The work ends with potential ideas for future work involving composite scaffolds for bone tissue engineering.

5.1 Bioglass 45S5 Transformation

The main part of this thesis is concerned with characterizing Bioglass 45S5 reactivity during scaffold processing. The analysis is conducted in four phases. The first consists of a literature review for the purposes of understanding the interplay between the different components involved in bone tissue engineering. This part gives an overview of tissue engineering and artificial extracellular matrices, bone structure, development, and modelling, the characteristics of an ideal scaffold for bone tissue engineering, both natural and synthetic materials currently used for scaffold fabrication, and finally scaffold processing techniques. With a full grasp of the subject at hand, a preliminary study of BG particles follows. This preliminary characterization involves both the as received BG, and BG treated in fluids involved in scaffold processing, which are acetone and water. The preliminary analysis of BG particle size, dissolution behavior, and surface chemical environment can then be compared with a similar one on BG extracted from the scaffold and delineate any transformation that occurred during scaffold development. In the third phase, composite, biodegradable PDLLA-BG scaffolds are made using the selected scaffold processing technique of solvent casting and particulate leaching. This step is followed by a fourth one involving BG extraction from the scaffold and its subsequent analysis and comparison with both treated and as received BG. The characterization techniques used in this study include particle sizing, pH measurements, ICP-OES, FTIR, and XPS spectroscopic techniques.

The preliminary BG study demonstrates that acetone does not alter BG physical or chemical properties, although the latter are affected by water in the leaching step of

scaffold processing. Furthermore, the stages of BG reactivity as proposed by L.L. Hench have been confirmed by monitoring ionic release of Ca, P, Na, and Si, and pH in dissolution experiments. We can conclude with the following points, the first and most important which is BG was found to start reacting during scaffold fabrication. Characterization of BG both before and after inclusion in the polymeric matrix of the scaffold demonstrates surface chemical transformations. Furthermore, the polymer is believed to provide a reactive environment for the Bioglass due to pH effects. Lastly, reactivity is influenced by Bioglass particle size.

5.2 Molding Material

A second enquiry arose while developing scaffolds for bone tissue engineering using the solvent casting and particulate leaching technique. Specifically, the Teflon mold used in the process to cast the paste was too rigid, making scaffold removal difficult. Teflon molds have been previously used in such applications because they are inert and do not raise concerns of reactivity with the polymeric filler used as scaffold material. However, the inflexibility of the Teflon mold produced scaffolds with non-uniform edges, which in many instances completely shattered because of the force induced during scaffold extraction. This second study therefore focused on finding a molding material, which must be flexible, but as we found out, even more important, must remain inert. In addition to Teflon, four materials were selected for appraisal: Sil940, a silicon-based molding material used in food-related application; polyurethane, another commonly used flexible molding material; polyether, a paste that quickly cures and is used in dentistry to mold teeth impressions; and finally polydimethylsiloxane (PDMS), another silicone-based

material with wide applicability in microfluidics components for biomedical applications. A PDLA film similar to the scaffolding paste was cast on the different materials to test the reactivity of each material, and characterized using XPS. All four materials were found to react with the PDLA solution, and released Si in the film. In an attempt to enhance material resistivity to the acetone used to dissolve PDLA, some materials (Sil940, polyether, PDMS) were treated (acetone, ethanol) or coated (Teflon spray, lacquer spray, Teflon tape, plasma). Plasma coated polyether was finally found to be both flexible and non-reactive with the acetone in the polymeric solution, and should hence be used in forthcoming studies to cast PDLA/acetone-based pastes to make scaffolds.

5.3 Suggestions for Future Work

This study brings up an interesting point, which is whether it would be desirable to produce a scaffold for bone tissue engineering that contains already reacted BG, perhaps even to the point where hydroxycarbonate apatite has precipitated on its surface.

An immediate investigation of the size-dependent dissolution behaviour of scaffold components or studies in simulated body fluid can provide further insight on the integration of multiple components within a single matrix.

In addition, the composite PDLA-BG scaffolds produced in this study can be further developed. For example, the hydrophobic scaffold surface can be turned into a “cell-friendly” environment through surface modification technique such as chemical hydrolysis/aminolysis, covalent immobilization or layer by layer self assembly of proteins. Finally, the shape and morphology of scaffolds made using the solvent

casting/particulate leaching method can be compared with scaffolds developed by alternative techniques such as electrospinning.

6 – References

- Albertsson, A.-C. (2002). *Degradable aliphatic polyesters*. Berlin ; London: Springer.
- Anderson, J. M., & Shive, M. S. (1997). Biodegradation and biocompatibility of PLA and PLGA microspheres. *Advanced Drug Delivery Reviews*, 28(1), 5-24.
- Atala, A. (2010). *Principles of regenerative medicine* (2nd ed. ed.). London: Academic.
- Auras, R. (2010). *Poly(lactic acid) : synthesis, structures, properties, processing, and applications*. Oxford: Wiley-Blackwell.
- Barbucci, R. (2002). *Integrated biomaterials science*. New York ; London: Kluwer Academic/Plenum.
- Behonick, D. J., & Werb, Z. (2003). A bit of give and take: the relationship between the extracellular matrix and the developing chondrocyte. *Mechanisms of Development*, 120(11), 1327-1336.
- Biber, M. V., & Stumm, W. (1994). An In-Situ ATR-FTIR Study: The Surface Coordination of Salicylic Acid on Aluminum and Iron(III) Oxides. *Environmental Science & Technology*, 28(5), 763-768.
- Bioavailability of contaminants in soils and sediments : processes, tools, and applications*. (2003). Washington, D.C.: National Academies Press.
- Boccaccini, A. R., & Maquet, V. (2003). Bioresorbable and bioactive polymer/Bioglass (R) composites with tailored pore structure for tissue engineering applications. *Composites Science and Technology*, 63(16), 2417-2429. doi: Doi 10.1016/S0266-3538(03)00275-6
- Boccafroschi, F., Habermehl, J., Vesentini, S., & Mantovani, D. (2005). Biological performances of collagen-based scaffolds for vascular tissue engineering. *Biomaterials*, 26(35), 7410-7417.
- Bökel, C., & Brown, N. H. (2002). Integrins in Development: Moving on, Responding to, and Sticking to the Extracellular Matrix. *Developmental Cell*, 3(3), 311-321.
- Briggs, D., & Grant, J. T. (2003). *Surface analysis by Auger and x-ray photoelectron spectroscopy*. Chichester: IM Publications.
- Bulstrode, C. J. K. (2010). *Oxford textbook of trauma and orthopaedics* (2nd ed.). Oxford: Oxford University Press.
- Burdick, J. A., Mauck, R. L., & SpringerLink. (2011). Biomaterials for Tissue Engineering Applications A Review of the Past and Future Trends Retrieved from <http://dx.doi.org/10.1007/978-3-7091-0385-2>
- Cerruti, M., Bianchi, C. L., Bonino, F., Damin, A., Perardi, A., & Morterra, C. (2005). Surface modifications of bioglass immersed in TRIS-buffered solution. A multitechnical spectroscopic study. *Journal of Physical Chemistry B*, 109(30), 14496-14505.
- Cerruti, M., Greenspan, D., & Powers, K. (2005). Effect of pH and ionic strength on the reactivity of Bioglass((R)) 45S5. *Biomaterials*, 26(14), 1665-1674.
- Chatterjee, K., Lin-Gibson, S., Wallace, W. E., Parekh, S. H., Lee, Y. J., Cicerone, M. T., Young, M.F., Simon, C. G., Jr. (2010). The effect of 3D hydrogel scaffold modulus on osteoblast differentiation and mineralization revealed by combinatorial screening. *Biomaterials*, 31(19), 5051-5062.
- Chu, P. K., & Liu, X. (2008). *Biomaterials fabrication and processing handbook*. Boca Raton, Fla.: CRC ; London : Taylor & Francis [distributor].

- Ducheyne, P., & Qiu, Q. (1999). Bioactive ceramics: the effect of surface reactivity on bone formation and bone cell function. *Biomaterials*, 20(23-24), 2287-2303.
- Dvir, T., Timko, B. P., Brigham, M. D., Naik, S. R., Karajanagi, S. S., Levy, O., Jin, H., Parker, K.K., Langer, R., Kohane, D. S. (2011). Nanowired three-dimensional cardiac patches. [10.1038/nnano.2011.160]. *Nat Nano*, 6(11), 720-725.
- Dvir, T., Timko, B. P., Kohane, D. S., & Langer, R. (2011). Nanotechnological strategies for engineering complex tissues. *Nat Nanotechnol*, 6(1), 13-22.
- ESPE, M. (2011). Impregum™ Soft Polyether Impression Material from <http://solutions.3m.com/>
- Giancotti, F. G., & Ruoslahti, E. (1999). Integrin Signaling. *Science*, 285(5430), 1028-1033.
- Greenspan, D. C., & Hench, L. L. (1976). Chemical and Mechanical-Behavior of Bioglass-Coated Alumina. *Journal of Biomedical Materials Research*, 10(4), 503-509.
- Guelcher, S. A., & Hollinger, J. O. (2006). *An introduction to biomaterials*. Boca Raton ; London: CRC/Taylor & Francis.
- Hench, L. L. (1977). Surface-Chemistry of Bioglass-Ceramic Implant Materials. *Abstracts of Papers of the American Chemical Society*, 173(Mar20), 10-10.
- Hench, L. L., Paschall, H. F., Paschall, M., & Mcvey, J. (1973). Histological Responses at Bioglass and Bioglass-Ceramic Interfaces. *American Ceramic Society Bulletin*, 52(4), 432-432.
- Herren, D. B., Nagy, L., Campbell, D., & Federation of European Societies for Surgery of the Hand. Meeting. (2008). *Osteosynthesis in the hand : current concepts : FESSH instructional course 2008*. Basel ; New York: Karger.
- Hollinger, J. O. (2005). *Bone tissue engineering*. Boca Raton, Fla. ; London: CRC.
- Hougham, G. (1999). *Fluoropolymers 2 : properties*. New York ; London: Kluwer Academic/Plenum.
- Hutmacher, D. W. (2000). Scaffolds in tissue engineering bone and cartilage. *Biomaterials*, 21(24), 2529-2543. doi: Doi: 10.1016/s0142-9612(00)00121-6
- Jones, E. (2010). Engineering principles in Physiological Systems. *The MusculoSkeletal System Part I* [CHEE 562 course powerpoint slides & notes]. Montreal.
- Karageorgiou, V., & Kaplan, D. (2005). Porosity of 3D biomaterial scaffolds and osteogenesis. *Biomaterials*, 26(27), 5474-5491.
- Khademhosseini, A., Vacanti, J. P., & Langer, R. (2009). Progress in tissue engineering. *Sci Am*, 300(5), 64-71.
- Kulin, R. M., Jiang, F., & Vecchio, K. S. (2011). Effects of age and loading rate on equine cortical bone failure. *Journal of the Mechanical Behavior of Biomedical Materials*, 4(1), 57-75.
- Lanza, R. P., Langer, R. S., & Vacanti, J. (2007). *Principles of tissue engineering* (3rd ed. ed.). London: Academic.
- Liao, C.-J., Chen, C.-F., Chen, J.-H., Chiang, S.-F., Lin, Y.-J., & Chang, K.-Y. (2002). Fabrication of porous biodegradable polymer scaffolds using a solvent merging/particulate leaching method. *Journal of Biomedical Materials Research*, 59(4), 676-681.
- Liu, X., & Ma, P. X. (2004). Polymeric Scaffolds for Bone Tissue Engineering. *Annals of Biomedical Engineering*, 32(3), 477-486. doi: 10.1023/B:ABME.0000017544.36001.8e
- Loh, A., Chester, J. F., & Taylor, R. S. (1993). PTFE bypass grafting to isolated popliteal segments in critical limb ischaemia. *Eur J Vasc Surg*, 7(1), 26-30.
- Lucas, G. L., Cooke, F. W., & Friis, E. (1998). *A primer of biomechanics*. New York: Springer.
- Ma, P. X., & Elisseeff, J. H. (2005). *Scaffolding in tissue engineering*. Boca Raton: Taylor&Francis.
- Magno, M. H. R., Kim, J., Srinivasan, A., McBride, S., Bolikal, D., Darr, A., Hollinger, J.O., Kohn, J. (2010). Synthesis, degradation and biocompatibility of tyrosine-derived polycarbonate scaffolds. *Journal of Materials Chemistry*, 20(40), 8885-8893.

- Mata, A., Fleischman, A., & Roy, S. (2005). Characterization of Polydimethylsiloxane (PDMS) Properties for Biomedical Micro/Nanosystems. *Biomedical Microdevices*, 7(4), 281-293.
- Meyer-Blaser, U., Handschel, J., Meyer, T., Wiesmann, H. P., & SpringerLink. (2009). Fundamentals of Tissue Engineering and Regenerative Medicine Retrieved from <http://dx.doi.org/10.1007/978-3-540-77755-7>
- Mikos, A. G., Thorsen, A. J., Czerwonka, L. A., Bao, Y., Langer, R., Winslow, D. N., & Vacanti, J. P. (1994). Preparation and Characterization of Poly(L-Lactic Acid) Foams. *Polymer*, 35(5), 1068-1077.
- Miller-Stephenson Chemical Company, I. (2011). PTFE Dry Film Lubricants.
- Nakamoto, K. (1986). *Infrared and Raman spectra of inorganic and coordination compounds* (4th ed. ed.). New York: Wiley.
- Narayan, R. (2009). *Biomedical materials*. New York: Springer.
- Oh, J. E., Nam, Y. S., Lee, K. H., & Park, T. G. (1999). Conjugation of drug to poly(D,L-lactic-co-glycolic acid) for controlled release from biodegradable microspheres. *Journal of Controlled Release*, 57(3), 269-280. doi: 10.1016/S0168-3659(98)00123-0
- Panetta, N. J., Gupta, D. M., & Longaker, M. T. (2009). Bone Tissue Engineering Scaffolds of Today and Tomorrow. *Journal of Craniofacial Surgery*, 20(5), 1531-1532.
- Patterson, J., Stayton, P. S., & Xingde, L. (2009). Characterization of the Degradation of PLGA Microspheres in Hyaluronic Acid Hydrogels by Optical Coherence Tomography. *Medical Imaging, IEEE Transactions on*, 28(1), 74-81.
- Payá, J., Monzó, J., Borrachero, M. V., Velázquez, S., & Bonilla, M. (2003). Determination of the pozzolanic activity of fluid catalytic cracking residue. Thermogravimetric analysis studies on FC3R–lime pastes. *Cement and Concrete Research*, 33(7), 1085-1091.
- Persidis, A. (2000). Tissue engineering. *Nat Biotech*.
- Plopper, G., McNamee, H., Dike, L., Bojanowski, K., & Ingber, D. (1995). Convergence of integrin and growth factor receptor signaling pathways within the focal adhesion complex. *Mol. Biol. Cell*, 6(10), 1349-1365.
- Professionals, G.-O. T. f. L. S. (Producer). (2008, 10 May 2011). Haversian System. [video] Retrieved from <http://www.youtube.com/watch?v=HUdwCvHZguM>
- Qin, L. (2007). *Advanced bioimaging technologies in assessment of the quality of bone and scaffold materials : techniques and applications*. Berlin: New York : Springer.
- Ratner, B. D. (2004). *Biomaterials science : an introduction to materials in medicine* (2nd ed. ed.). Amsterdam ; London: Elsevier Academic Press.
- Robinson, J. W. (1995). *Undergraduate instrumental analysis* (5th ed rev. and expanded. ed.). New York: M. Dekker.
- Ruppel, M., Miller, L., & Burr, D. (2008). The effect of the microscopic and nanoscale structure on bone fragility. *Osteoporosis International*, 19(9), 1251-1265.
- Sabir, M. I., Xu, X. X., & Li, L. (2009). A review on biodegradable polymeric materials for bone tissue engineering applications. *Journal of Materials Science*, 44(21), 5713-5724.
- Salerno, A., Di Maio, E., Iannace, S., & Netti, P. (2011). Tailoring the pore structure of PCL scaffolds for tissue engineering prepared via gas foaming of multi-phase blends. *Journal of Porous Materials*, 1-8.
- Santin, M. (2008). *Strategies in regenerative medicine : integrating biology with materials design*. New York: Springer.
- Seol, Y. J., Lee, J. Y., Park, Y. J., Lee, Y. M., Young-Ku, Rhyu, I. C., Lee, S.J., Han, S.B., Chung, C. P. (2004). Chitosan sponges as tissue engineering scaffolds for bone formation. *Biotechnology Letters*, 26(13), 1037-1041.

- Shunji, Y., & et al. (2011). Effects of increased collagen-matrix density on the mechanical properties and in vivo absorbability of hydroxyapatite–collagen composites as artificial bone materials. *Biomedical Materials*, 6(1), 015012.
- Smooth-On, I. (2011a). ReoFlex® - Next Generation Urethane Rubber, 2011, from <http://www.smooth-on.com/>
- Smooth-On, I. (2011b). Smooth-Sil® 940 Suitable For Food-Related Applications, 2011, from www.smooth-on.com/
- SpillTech. (2011). Chemical Compatibility Guide For Polyurethane Items, 2011, from <https://www.spilltech.com/wcsstore/SpillTechUSCatalogAssetStore/Attachment/documents/ccg/POLYURETHANE.pdf>
- Stanfield, C. L., & Germann, W. J. (2009). *Principles of human physiology* (3rd ed. ed.). San Francisco: Pearson/Benjamin Cummings.
- Stevens, B., Yang, Y. Z., MohandaS, A., Stucker, B., & Nguyen, K. T. (2008). A review of materials, fabrication to enhance bone regeneration in methods, and strategies used engineered bone tissues. *Journal of Biomedical Materials Research Part B-Applied Biomaterials*, 85B(2), 573-582.
- Stevens, M. M., & George, J. H. (2005). Exploring and engineering the cell surface interface. *Science*, 310(5751), 1135-1138.
- Streuli, C. (1999). Extracellular matrix remodelling and cellular differentiation. *Curr Opin Cell Biol*, 11(5), 634-640.
- Suh, S. W., Shin, J. Y., Kim, J., Kim, J., Beak, C. H., Kim, D.-I., Kim, H., Jeon, S.S., Choo, I.-W. (2002). Effect of Different Particles on Cell Proliferation in Polymer Scaffolds Using a Solvent-Casting and Particulate Leaching Technique. *ASAIO Journal*, 48(5), 460-464.
- Tabrizian, M. (2011). Biomaterials & Bioperformance BMDE 504 lecture Montreal.
- Taipale, J., & Keski-Oja, J. (1997). Growth factors in the extracellular matrix. *The FASEB Journal*, 11(1), 51-59.
- Tran, K. T., Lamb, P., & Deng, J.-S. (2005). Matrikines and matricryptins: Implications for cutaneous cancers and skin repair. *Journal of Dermatological Science*, 40(1), 11-20.
- Vadgama, P. (2005). *Surfaces and interfaces for biomaterials*. Cambridge: Woodhead.
- Wainwright, S. A. (1982). *Mechanical design in organisms*. Princeton ; Guildford: Princeton University Press.
- Wnek, G. E., & Bowlin, G. L. (2004). *Encyclopedia of biomaterials and biomedical engineering*. New York: Marcel Dekker ; [London : Taylor & Francis].
- Xue, L., & Greisler, H. P. (2003). Biomaterials in the development and future of vascular grafts. *Journal of Vascular Surgery*, 37(2), 472-480.

7 – Appendices

Appendix A

Bioglass 45S5 Particle Sizing

Fig. A.1 – Particle Sizing Raw Data for the Three Trials of As Received BGA

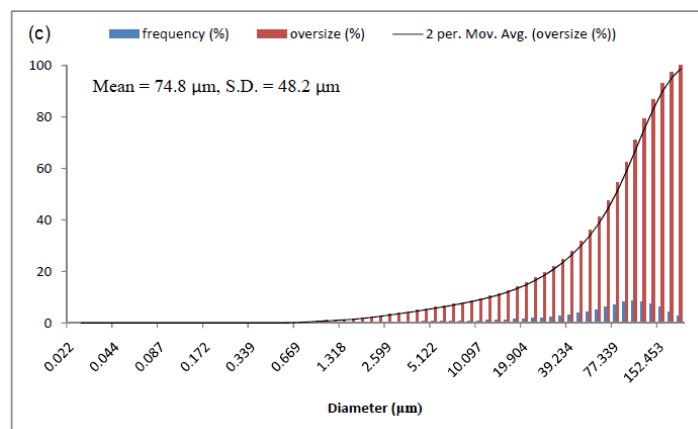
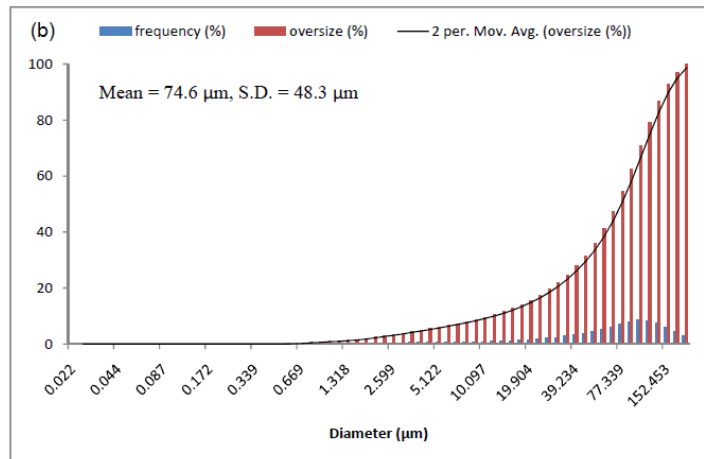
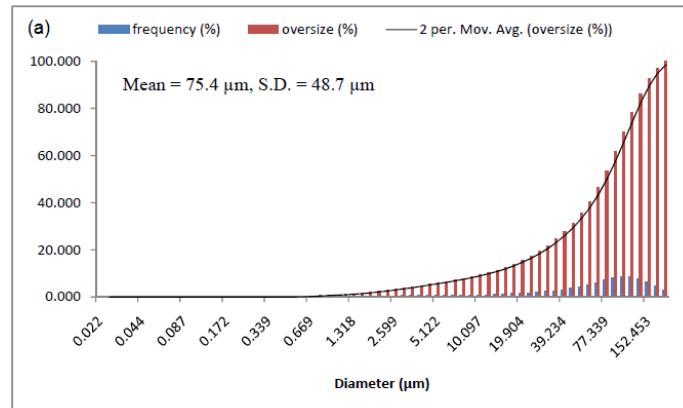


Fig. A.2 – Particle Sizing Raw Data for the Three Trials of As Received BGB

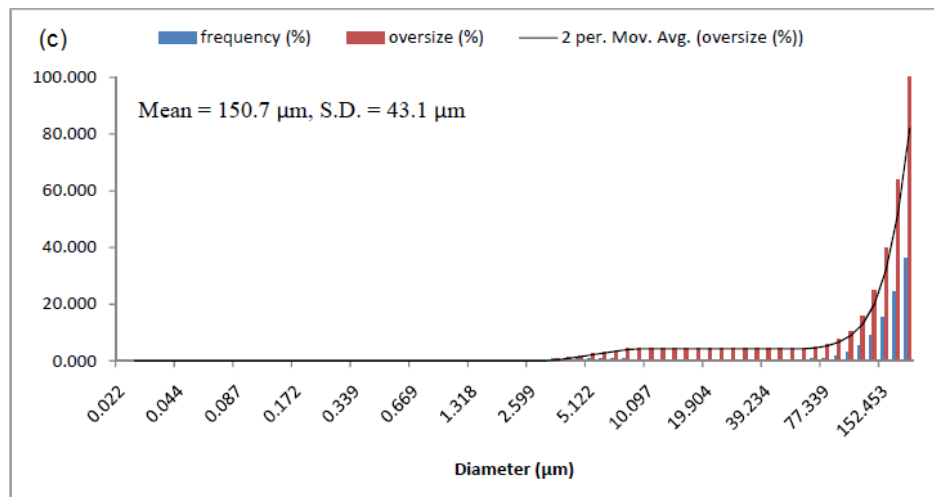
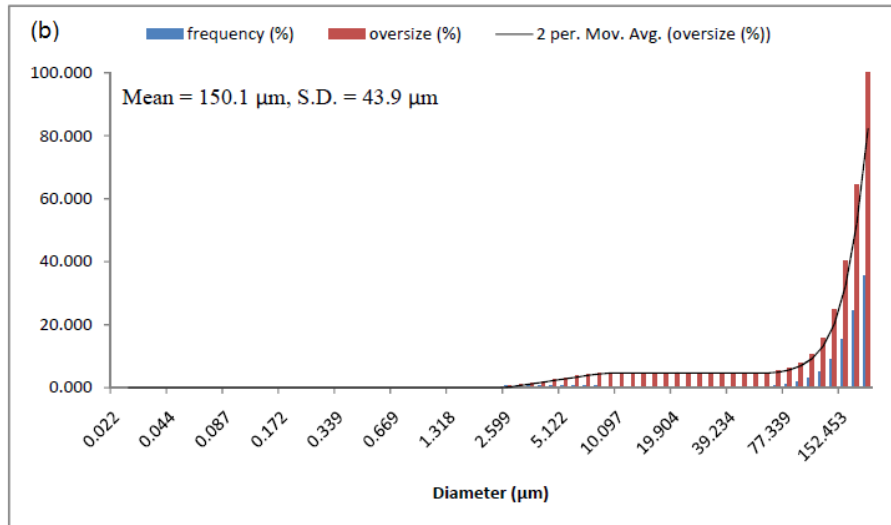
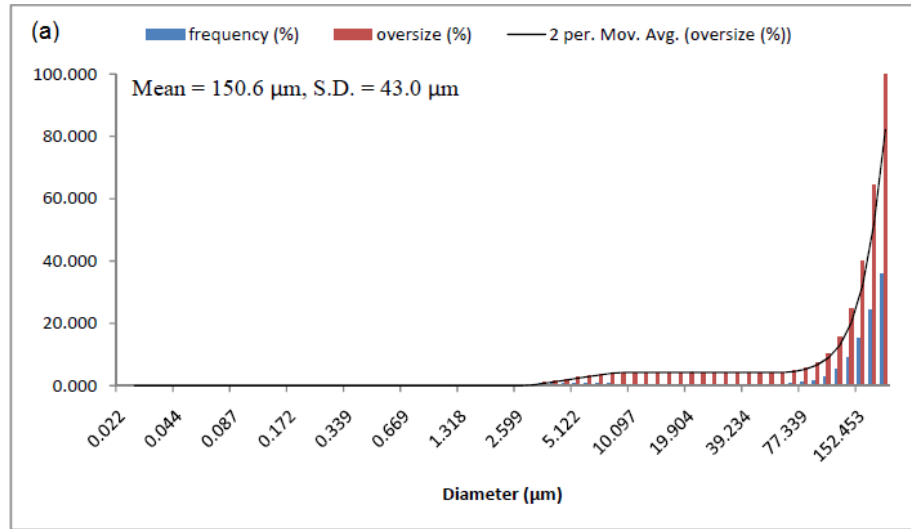


Fig. A.3 – Particle Sizing Raw Data for the Two Trials of Water Treated BGA

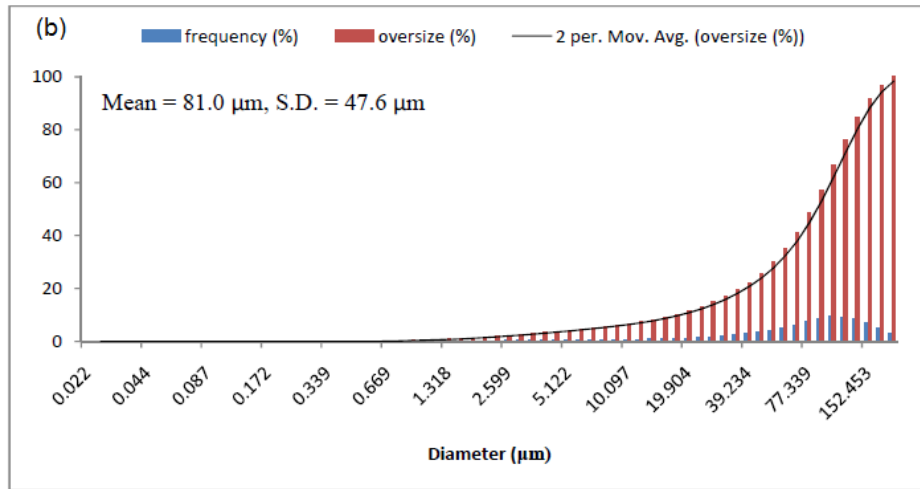
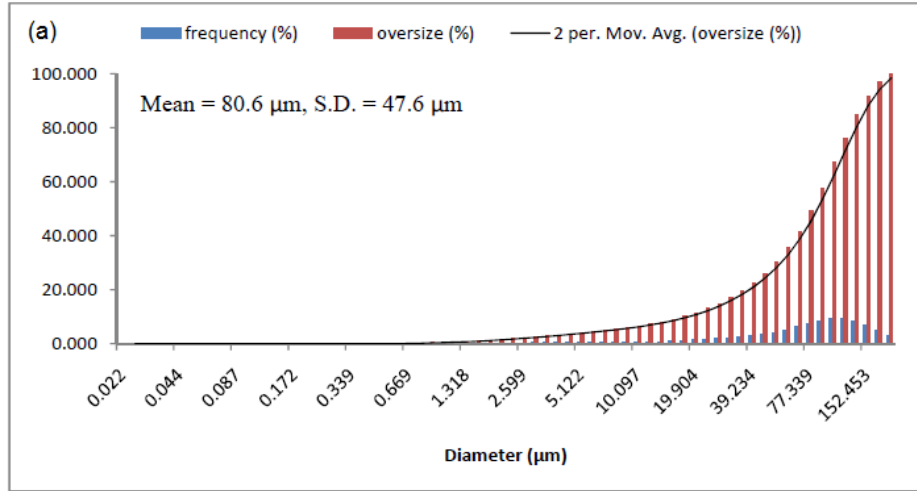


Fig. A.4 – Particle Sizing Raw Data for the Water Treated BGB

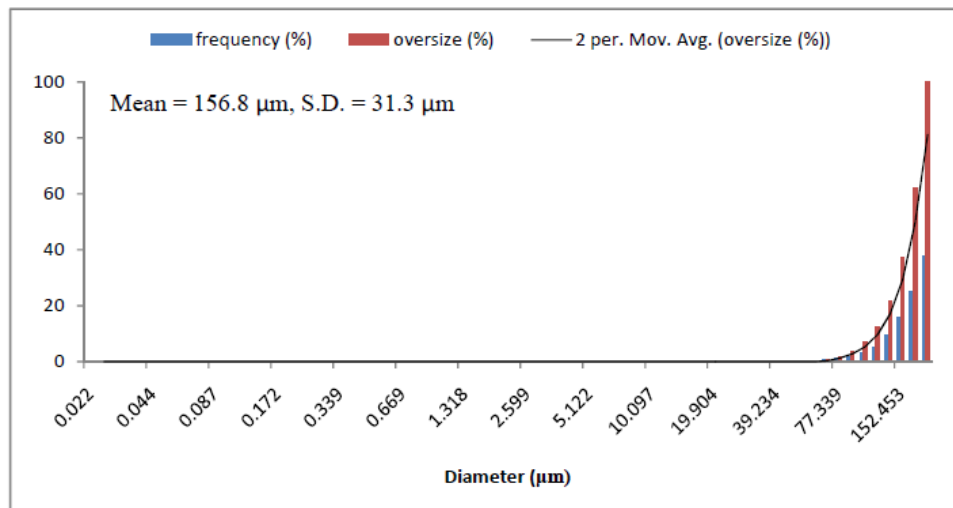


Fig. A.5 – Particle Sizing Raw Data for the Two Trials of Acetone Treated BGA

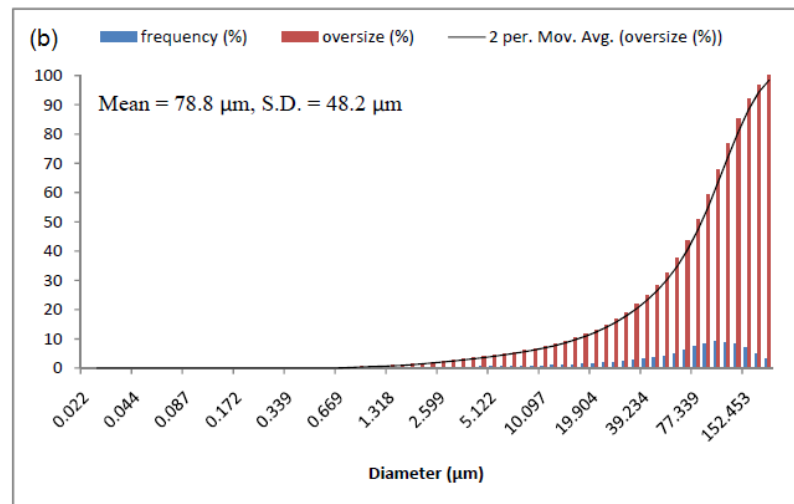
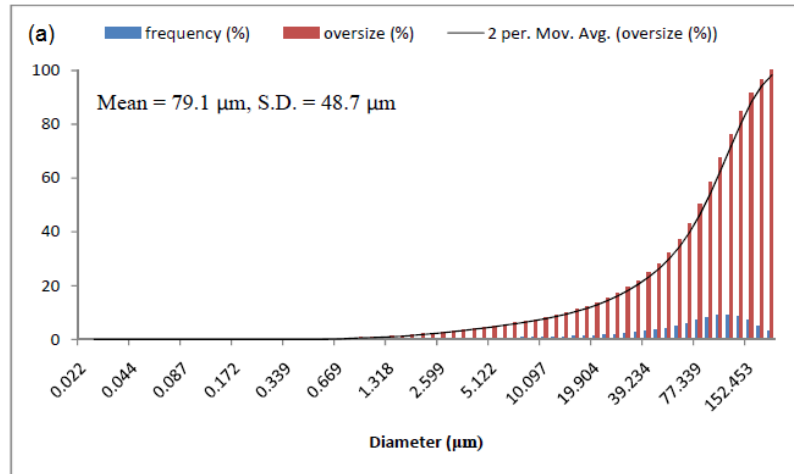


Fig. A.6 – Particle Sizing Raw Data for the Acetone Treated BGB

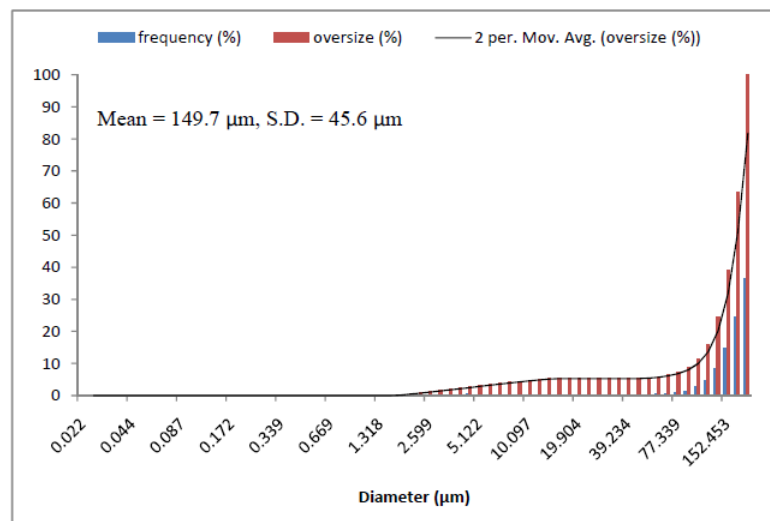


Fig. A.7 – Particle Sizing for the Two Trials of both Acetone & Water Treated BGA

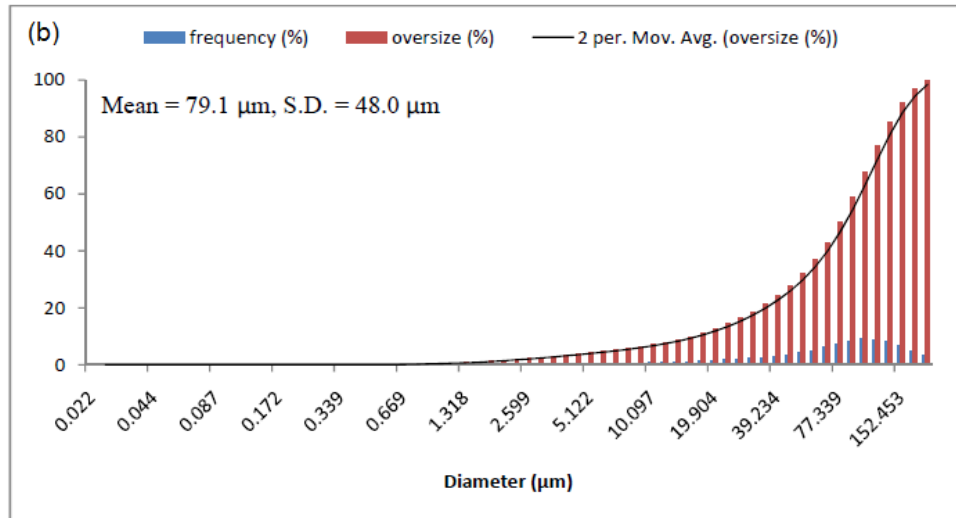
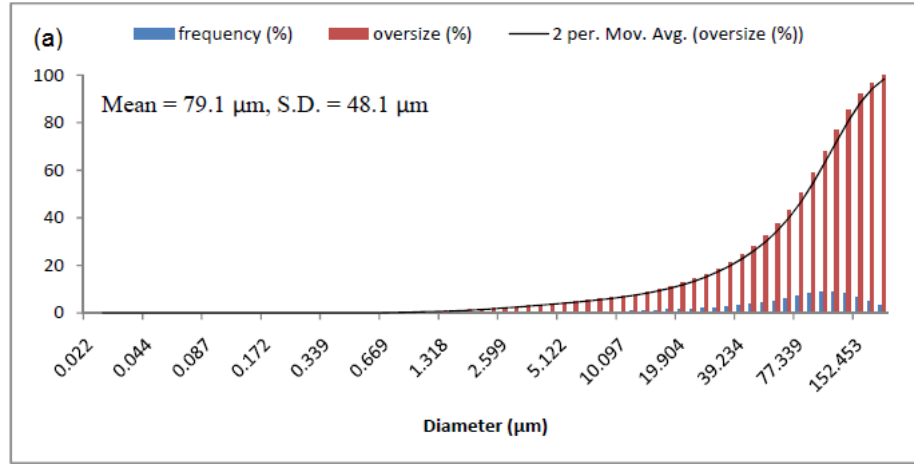
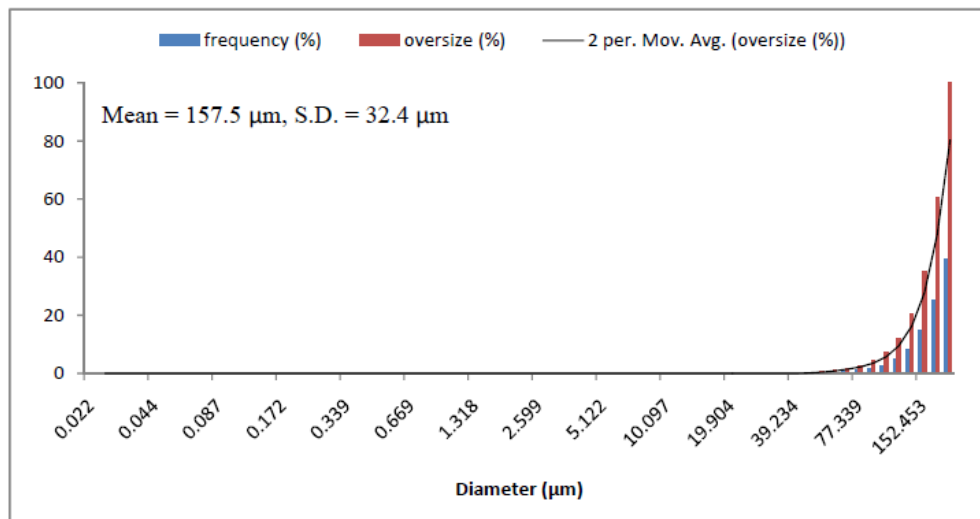


Fig. A.8 – Particle Sizing Raw Data for both Acetone & Water Treated BGB



Appendix B

XPS Characterization

of Molding Materials

Fig. B.1 – XPS Elemental Survey of PDLLA Film Cast on Si1940 Substrate, 3 Trials

1st Trial:

Name	Peak BE	FWHM eV	Area (P) CPS.eV	At. %
O1s	533.32	3.14	89304.52	25.88
C1s	285.91	3.16	65687.50	48.57
Si2p	103.84	3.15	30721.07	25.55

2nd Trial:

Name	Peak BE	FWHM eV	Area (P) CPS.eV	At. %
O1s	534.31	3.69	119828.31	29.13
C1s	286.51	2.53	87976.51	54.54
Si2p	104.35	3.24	23417.27	16.33

3rd Trial:

Name	Peak BE	FWHM eV	Area (P) CPS.eV	At. %
O1s	534.03	3.05	42058.12	28.39
C1s	285.43	3.45	30826.55	53.04
Si2p	103.96	2.80	9593.92	18.57

Fig. B.2 – High Resolution XPS Si Peak of Polyether Cast PDLLA Film, 3 Trials

Energies are miscalibrated due to surface charging.

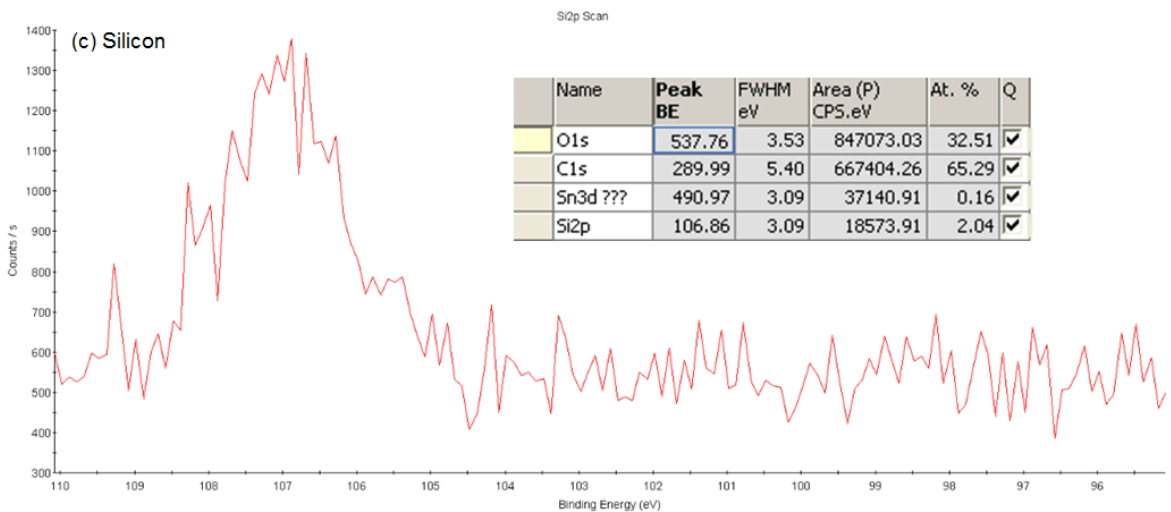
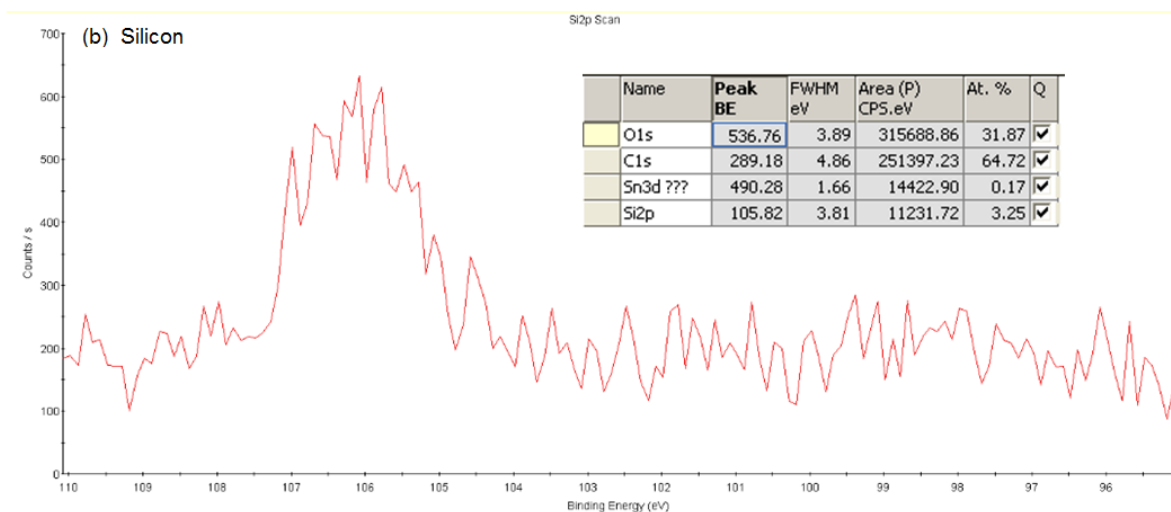
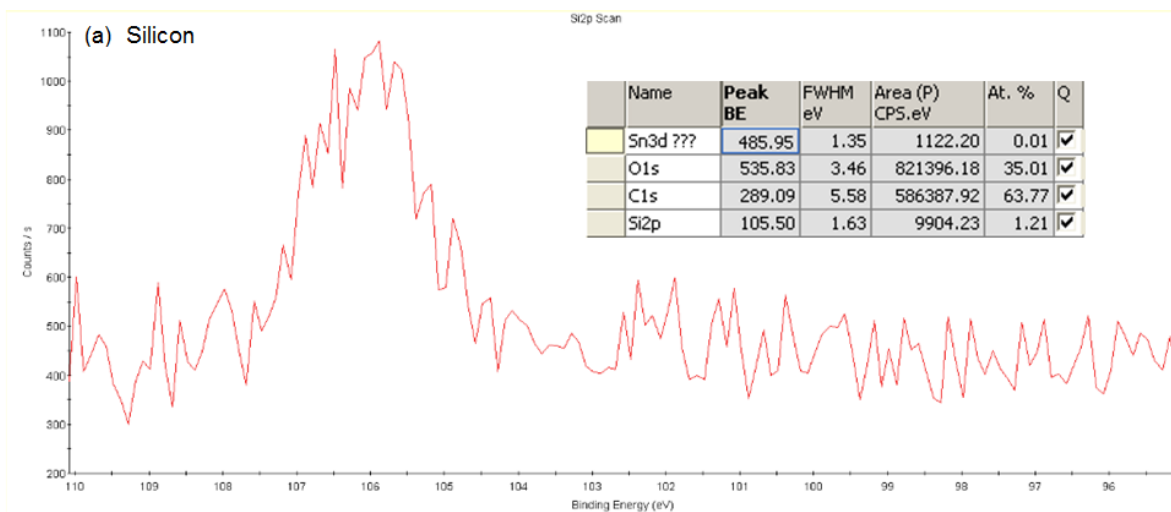


Fig. B.3 – XPS Survey of PDLLA Film made on PDMS, 3 Trials

1st Trial:

Name	Peak BE	FWHM eV	Area (P) CPS.eV	At. %
O1s	534.95	3.64	395697.70	31.51
C1s	287.33	4.33	263121.85	53.43
Si2p	105.13	3.12	65978.90	15.06

2nd Trial:

Name	Peak BE	FWHM eV	Area (P) CPS.eV	At. %
O1s	535.02	3.63	469236.65	32.45
C1s	287.30	4.38	308300.46	54.37
Si2p	105.05	3.05	65696.36	13.03
In3d	449.64	1.87	17204.17	0.15

3rd Trial:

Name	Peak BE	FWHM eV	Area (P) CPS.eV	At. %
O1s	535.87	3.59	415757.51	31.56
C1s	288.04	4.68	283752.34	54.92
Si2p	105.37	3.02	62107.20	13.51

Fig. B.4 – XPS Survey of PDLLA Film made on Acetone Treated PDMS, 2 Trials

